STOCHASTIC STEEPEST DESCENT WITH ACCELERATION FOR ℓ_p-SMOOTH NON-CONVEX OPTIMIZATION

Anonymous authors
Paper under double-blind review

ABSTRACT

In this work, we analyze stochastic ℓ_p steepest descent for non-convex problems. Specifically, for $p > 2$, we establish ϵ-approximate stationarity (in expectation) with respect to the dual norm $\|\cdot\|_{p^*}^{p^*}$ at a rate of $O(\epsilon^{-4})$, thereby generalizing the previous guarantees for signSGD ($p = \infty$). In addition, inspired by techniques for the convex setting, we present a new *accelerated* ℓ_p descent method, called STACEY, based on interpolated primal-dual iterate sequences that are designed for non-Euclidean smooth optimization settings. We compare our algorithm against popular methods such as SGD, Adam, AdamW, and Lion on image classification and pretraining language modeling tasks, and our results demonstrate the potential for both faster convergence and achieving higher accuracy. We further evaluate our algorithm for different values of p across various models and datasets, highlighting the importance and efficiency of non-Euclidean methods as compared to standard Euclidean-based approaches.[1]

1 INTRODUCTION

Stochastic first-order methods have proven essential for efficiently training modern deep learning models. In addition to the basic stochastic gradient descent (SGD) algorithm (Robbins & Monro, 1951)—along with its momentum-based variants (Nesterov, 1983; Polyak, 1964)—other methods, such as AdaGrad (Duchi et al., 2011), Adam (Kingma, 2014), and AdamW (Loshchilov & Hutter, 2019), incorporate second moment gradient information to provide per-coordinate scaling, and the use of these adaptive techniques has since become standard for optimizing deep neural networks.

A related approach involves updating the parameters based on the *sign* of the (stochastic) gradient (Balles et al., 2020; Bernstein et al., 2018; Riedmiller & Braun, 1992). For example, the Lion method (Chen et al., 2023)—discovered symbolically through a program search—combines the sign-based step with a certain momentum scheme (which differs from that of the Signum method (Bernstein et al., 2018)), and more recently, the Lion-$\mathcal{K}$ method (Chen et al., 2024) establishes a family of methods—for which Lion is a special case—defined in terms of a general convex function $\mathcal{K}(\cdot)$. These algorithms have been shown to be competitive with—and in some cases even outperform—popular adaptive methods, particularly for large language models.

Guarantees for non-convex optimization. Given the empirical success of sign-based methods, we may then naturally ask *why* they perform as well as they do.[2] Although globally optimizing non-convex problems is NP-hard in general, one may nevertheless instead consider the relaxed goal of reaching approximate stationary points—sometimes strengthened to that of finding approximate local minima (Agarwal et al., 2017; Carmon et al., 2018; Ge et al., 2015)—for both deterministic (Carmon et al., 2017) and stochastic (Ghadimi & Lan, 2013) first-order methods. However, crucial to these guarantees (and their limitations) are the assumptions we make, notable among them being that the function is *smooth*, and there additionally lies behind these notions of stationarity (and smoothness) *a particular choice of norm*.

[1] The code is included in the supplementary material and will be publicly available upon acceptance.

[2] Indeed, understanding the dynamics—not to mention issues of generalization—for deep learning optimization has been the subject of significant effort (e.g., (Allen-Zhu et al., 2019a;b; Arora et al., 2019a;b; Du et al., 2017; 2018; 2019; Gunasekar et al., 2018a;b; Jacot et al., 2018; Jin et al., 2017; Soudry et al., 2018; Ward et al., 2020; Wilson et al., 2017)), such that a complete accounting is beyond the scope of this paper.

For example, in the case of SGD, Ghadimi & Lan (2013) establish approximate stationarity guarantees of the form $\mathbb{E}[\|\nabla f(\hat{x})\|_2] \leq \epsilon$ (where $\|\cdot\|_2$ denotes the standard Euclidean norm) under a smoothness assumption similarly defined with respect to $\|\cdot\|_2$. On the other hand, Bernstein et al. (2018) show how signSGD—which we may also view as (unscaled) stochastic steepest descent w.r.t. $\|\cdot\|_\infty$—can guarantee that $\mathbb{E}[\|\nabla f(\hat{x})\|_1] \leq \epsilon$, under a particular ℓ_2 majorization assumption (which, as we discuss further in Appendix B, implies *smoothness w.r.t.* $\|\cdot\|_\infty$ (Balles et al., 2020)).

Stochastic ℓ_p descent. Taken together, these two examples—albeit from opposite ends of the (norm) spectrum—suggest a fundamental interplay between the (primal) norm that is the basis of the *steepest descent* iteration (paired with smoothness defined in terms of the same norm) and the (dual) norm used to measure approximate stationarity. Previous works, however, have focused on either the case of stochastic steepest descent w.r.t. $\|\cdot\|_p$ for $p = 2$ (SGD) or $p = \infty$ (signSGD), or else depend on unconventional noise assumptions (Carlson et al., 2015), thus leaving open the question—which we address in Section 3—of extending these results to all $2 < p < \infty$ under standard variance assumptions.

While at first glance this may appear to be a straightforward extension, in fact several technical challenges arise when generalizing the analysis under ℓ_p smoothness assumptions, among them the fact that the stochastic coordinate-wise scaled step is not an unbiased estimator of the (deterministic) steepest descent direction (as for $p = 2$), nor is the magnitude the same across all coordinates of each step (as for $p = \infty$).[3] Indeed, extensions of this sort, in terms of general ℓ_p norms, for minimizing the dual norm of the gradient have been addressed in the deterministic, convex setting (Diakonikolas & Guzmán, 2024) (as have related questions for minimizing the optimality gap (Guzmán & Nemirovski, 2015; Nemirovskii & Nesterov, 1985)), and so our results provide a natural counterpart for the stochastic, non-convex setting.

Even so, one may reasonably ask: *why should we ever be concerned with any p other than* 2 *or* ∞*?*

Problem geometry and acceleration. In fact, we believe a key observation here lies in determining the *appropriate geometry* for the problem at hand, most clearly reflected in not only the choice of norm used for measuring smoothness, *but also the magnitude of the smoothness parameter itself.*[4] (This is naturally to be balanced against the different dual norms—e.g., $\|\nabla f(\hat{x})\|_2$ for $p = 2$ vs. $\|\nabla f(\hat{x})\|_1$ for $p = \infty$—used to define approximate stationarity.) Unfortunately, it can be difficult to determine the precise smoothness parameters w.r.t. general ℓ_p norms (Balles et al., 2020); nevertheless, there is ample evidence (e.g., Adolphs et al. (2019); Becker et al. (1988); Cohen et al. (2021a); Ghorbani et al. (2019); Jiang et al. (2024); Li et al. (2020); Li & Zhang (2024); Papyan (2018))—including empirical results of our own, as we later present in Section 5—to suggest that a different choice of p (outside of 2 or ∞) could allow for better adapting to the structure of certain (deep learning) objectives.

As a complement to this matter of defining (and parameterizing) smoothness, however, there arises a second lens through which we observe the potential for general p, *namely that of acceleration* (Allen-Zhu & Orecchia, 2017; Bai & Bullins, 2024; Nemirovskii & Nesterov, 1985; Nesterov, 1983; 2005). Though we provide a more thorough overview in Section 4, there is, in essence, a fundamental trade-off (for convex settings) between the rate of acceleration and the norm used to measure the initial distance to the optimal solution. Concretely, it is well known that, for convex $f(x)$ that is L-smooth *with respect to* $\|\cdot\|_2$, the classic accelerated gradient descent (AGD) method of Nesterov (1983) converges at the rate $f(x_T) - f(x^*) \leq O\left(\frac{L\|x_0 - x^*\|_2^2}{T^2}\right)$, and this rate is indeed tight (Nesterov,

[3] Although stochastic mirror descent (S-MD) can provide guarantees (in terms of minimizing optimality gap, e.g., (Bubeck et al., 2015), Theorem 6.1) under smoothness w.r.t. a general norm $\|\cdot\|$, we would note that doing so requires the mirror map to be strongly convex w.r.t. $\|\cdot\|$, which leads to certain basic difficulties in optimization theory when considering $\|\cdot\|_p$ for $p > 2$. (We refer the reader to, e.g., (Cohen et al., 2021b; Kelner et al., 2014; Sherman, 2017; Sidford & Tian, 2018), for additional details.) This point likewise suggests what is a key difference between *steepest* and *mirror* descent (as also reflected in our analysis versus that of S-MD), the exploration of which yields interesting consequences for appropriately accelerating in *non-Euclidean* settings (Allen-Zhu & Orecchia, 2017), as we discuss in Section 4.

[4] We may note that, for all $2 \leq \gamma \leq \delta$, being L_δ-smooth w.r.t. $\|\cdot\|_\delta$ implies being L_δ-smooth w.r.t. $\|\cdot\|_\gamma$, whereas being L_γ-smooth w.r.t. $\|\cdot\|_\gamma$ implies being $d^{\frac{2}{\gamma}-\frac{2}{\delta}} L_\gamma$-smooth w.r.t. $\|\cdot\|_\delta$.

2018; Nemirovskij & Yudin, 1983). Importantly, we emphasize the appearance here of $\|\cdot\|_2$ for both the measure of smoothness *as well as* the $\|x_0 - x^*\|_2^2$ term.

Trade-offs for non-Euclidean acceleration. Based on the discussion so far, it would then be only natural to ask whether the accelerated rates of AGD hold under general smoothness assumptions. Unfortunately, the standard analysis of AGD does not readily adapt to alternative notions of smoothness, as the design of the algorithm is, in a sense, *specific to Euclidean settings*; we refer the reader to the work of Allen-Zhu & Orecchia (2017) for further discussion of this basic incompatibility. Nevertheless, several works (Diakonikolas & Guzmán, 2024; Nemirovskii & Nesterov, 1985; Nesterov, 2005; Song et al., 2019)—including that of Allen-Zhu & Orecchia (2017)—have provided techniques for *accelerating in non-Euclidean settings*, whereby common among them is, roughly speaking, a certain type of primal-dual coupling/interpolation. In particular, the approach of Nemirovskii & Nesterov (1985), for convex $f(x)$ that is L-smooth *with respect to* $\|\cdot\|_p$, leads to guarantees of the form

$$f(x_T) - f(x^*) \leq O\left(\frac{L\|x_0 - x^*\|_p^2}{T^{\frac{p+2}{p}}}\right). \tag{1}$$

(See also, e.g., Theorem 2 in (Diakonikolas & Guzmán, 2024).) Moreover, these rates are similarly known to be tight (Guzmán & Nemirovski, 2015).

Looking closely at these convergence guarantees, we may first note that, for $p = 2$, the rate in equation 1 recovers that of Nesterov (1983). On the other hand, for $p \to \infty$, while $\|x_0 - x^*\|_p^2$ can, at best, be as small as $d^{\frac{2}{p}-1}\|x_0 - x^*\|_2^2$, we also have that $\lim_{p\to\infty} T^{-\frac{p+2}{p}} = T^{-1}$—*in which case the benefit of acceleration disappears altogether*—and in fact this (limiting) rate essentially matches that of *unaccelerated* ℓ_∞ steepest descent (Kelner et al., 2014).

Consequently, these observations reveal the opportunity afforded by (non-Euclidean) ℓ_p-based accelerated methods in the form of this trade-off between the *dependence on the problem geometry* and the *rate of acceleration*. As a further illustration, if we consider, e.g., $p = 4$, there is a (potential) gain of up to a $d^{1/2}$ factor (resulting from the $\|\cdot\|_4^2$ term) compared to the standard Euclidean ($p = 2$) case, whereas the rate of acceleration would degrade from T^{-2} to $T^{-3/2}$.

Practical considerations. We acknowledge, of course, that these results are for convex problems, whereas in this work we focus on the non-convex setting.[5] Nevertheless, we would argue there is a well-established pattern (Agarwal et al., 2019; Dozat, 2016; Gupta et al., 2018; Kingma, 2014; Liu et al., 2020; 2024; Reddi et al., 2018; Sutskever et al., 2013; Zeiler, 2012) of designing deep learning optimizers in a manner inspired by those analyzed for *convex* settings (Boyd & Vandenberghe, 2004; Bubeck et al., 2015; Duchi et al., 2011; Nemirovskij & Yudin, 1983; Nesterov, 1983; Polyak, 1964; Robbins & Monro, 1951), and so we also work from such a starting point—our own inspiration drawing from *non-Euclidean* methods—in developing our new accelerated algorithm STACEY (**St**ochastic **St**eepest Descent with **Acce**leration), which we discuss further in Section 4.

1.1 Contributions and Paper Overview

As a whole, the aim of this work is to examine more carefully the opportunities for non-convex problems *whose geometry is amenable to ℓ_p norm-based algorithms*. To this end, we begin by addressing in Section 3 the question of reaching ϵ-approximate stationarity under general ℓ_p smoothness assumptions, whereby we establish, for $2 < p < \infty$, convergence guarantees of the form $E[\|\nabla f(\hat{x})\|_{p^*}^{p^*}] \leq \epsilon$ after $O(\epsilon^{-4})$ iterations of the stochastic ℓ_p descent algorithm (where we let $p^* := \frac{p}{p-1}$). We then present, in Section 4, our algorithm STACEY, which provides for *accelerating* these (stochastic) ℓ_p descent methods, based on a primal-dual interpolation of gradient and mirror descent steps. Finally, we observe the promising empirical performance of STACEY in Section 5, as demonstrated via both synthetic examples and large-scale image classification and pretraining language modeling tasks.

[5] In fact, under standard assumptions on the non-convex function (i.e., smoothness and being bounded from below) and the stochastic gradient oracle (i.e., that it is provides an unbiased estimator of the gradient with bounded variance), known lower bounds establish that, without additional assumptions, *acceleration is not attainable in general* (Arjevani et al., 2023; Carmon et al., 2020; 2021).

Algorithm 1 Stochastic ℓ_p Descent

```
    input $p, \eta, f, \theta_0$
1:  for $t = 0$ to $T - 1$ do
2:      $\theta_{t+1} = \theta_t - \eta s\left(g(\theta_t)\right)$      ▷ $s(x) = [s_1(x), \cdots, s_d(x)]^\top$ where $s_i(x) = \frac{x^{(i)}}{|x^{(i)}|^{\frac{p-2}{p-1}}}$
    return $\theta_T$
```

2 Preliminaries and Assumptions

Throughout we let $\|\cdot\|$ and $\|\cdot\|_*$ denote a general norm and its dual, respectively. In addition, we specify $\|\cdot\|_p$ to denote the standard ℓ_p norm ($1 \leq p \leq \infty$) and $\|\cdot\|_{p^*} := \|\cdot\|_{p/(p-1)}$ to denote its dual norm. For symmetric $M \in \mathbb{R}^{d\times d}$ s.t. $M \succ 0$, we further let $\|\cdot\|_M$ denote the standard matrix norm, i.e., $\|x\|_M = \sqrt{x^\top Mx}$ for $x \in R^d$. For a vector $v \in \mathbb{R}^d$, we use superscript, i.e., $v^{(i)}$ to denote the i^{th} coordinate of v, and we let diag(v) denote the diagonal matrix such that diag$(v)_{i,i} = v^{(i)}$. We use subscript, e.g., θ_t, to denote a vector in the t^{th} iteration.

It will be useful for our analysis to consider certain basic regularity assumptions, such as that of smoothness.

Definition 1 (Smoothness)**.** *We say a function $f : \mathbb{R}^d \mapsto \mathbb{R}$ is L-smooth w.r.t. $\|\cdot\|$ if, for all $x, y \in \mathbb{R}^d$, $\|\nabla f(y) - \nabla f(x)\|_* \leq \|y - x\|$.*

Equivalently, we have the following.

Assumption 1 (Smoothness in ℓ_p norm)**.** *Let $f : \mathbb{R}^d \mapsto \mathbb{R}$ be L-smooth w.r.t. $\|\cdot\|_p$ for $p \geq 2$. Then, for all $x, y \in \mathbb{R}^d$,*

$$\left|f(y) - f(x) - \nabla f(x)^\top (y - x)\right| \leq \frac{L}{2}\|y - x\|_p^2.$$

Assumption 2 (Unbiased Estimate)**.** *The stochastic gradient $g(x)$ is an unbiased estimate of the true gradient $\nabla f(x)$. That is, $\mathbb{E}[g(x)] = \nabla f(x)$.*

Assumption 3 (Bounded Variance)**.** *For some data ξ, the variance of each coordinate of the stochastic gradient is bounded, i.e., $\forall i \in [d]$, $\mathbb{E}[|g(x)^{(i)} - \nabla f(x)^{(i)}|^2] \leq \sigma_i^2$.*

Corollary 1. *By Assumption 3, $\mathbb{E}[\|g(x) - \nabla f(x)\|_2^2] \leq \sigma^2$ where for $\sigma := \|\vec{\sigma}\|_2$, $\vec{\sigma} = [\sigma_1, \cdots, \sigma_d]^\top$.*

Corollary 2. *If the stochastic gradient is an n-sample mini-batch estimate, then $\forall i \in [d]$, $\mathbb{E}[|g(x)^{(i)} - \nabla f(x)^{(i)}|^2] \leq \frac{\sigma_i^2}{n}$.*

Assumption 4 (Bounded gradient)**.** *For $G > 0$, $p \geq 2$, and p^* where $\frac{1}{p} + \frac{1}{p^*} = 1$, $\|g(x)\|_{p^*} \leq G$.*

Corollary 3. *By Assumption 4, we know that*

(a) $\|\nabla f(x)\|_{p^*} = \|\mathbb{E}\left[g(x)\right]\|_{p^*} \leq \mathbb{E}\left[\|g(x)\|_{p^*}\right] \leq G$ with Jensen's inequality.

(b) $\forall\, i \in [d]$, $\left|g(x)^{(i)}\right| \leq G$ and $\left|\nabla f(x)^{(i)}\right| \leq G$.

3 Convergence for Stochastic ℓ_p Descent

In this section, we present the stochastic ℓ_p descent algorithm and analyze its convergence. As demonstrated in Algorithm 1, the update step takes the unscaled form [6] of its counterpart in the deterministic setting $\theta_{t+1}^{(i)} = \theta_t^{(i)} - \eta\|f(\theta_t)\|_{p^*}^{\frac{p-2}{p-1}} \frac{f(\theta_t)^{(i)}}{\left|f(\theta_t)^{(i)}\right|^{\frac{p-2}{p-1}}}$ (Bai & Bullins, 2024), which is derived from the closed form of $\theta_{t+1} = \arg\min_\theta \left\{\langle \eta f\left(\theta_t\right), \theta - \theta_t\rangle + \frac{1}{2}\|\theta - \theta_t\|_p^2\right\}$. When $p = \infty$, Algorithm 1 reduces exactly to signSGD (Bernstein et al., 2018).

For $p > 2$, we show in Theorem 1 that stochastic ℓ_p descent converges in expectation to an ϵ-approximate stationary point with respect to the dual norm at a rate of $O(\epsilon^{-4})$, thereby generalizing

[6] This is in line with signSGD (Bernstein et al., 2018) compared to the scaled form in (Balles et al., 2020). In addition, we adopt the unscaled version for clearer convergence analysis and more practical implementation.

the previous guarantees for signSGD ($p = \infty$). In addition, we provide a proof sketch, deferring the complete proof to Appendix A.1. Curiously, as we will see, moving from the ℓ_2 setting (or even from the ℓ_∞ setting) introduces certain technical considerations that need to be addressed non-trivially.

Theorem 1 (Main)**.** *Running Algorithm 1 on some (possibly non-convex) function f that satisfies Assumptions 1 to 4 yields*

$$\mathbb{E}\left[\frac{1}{T}\sum_{t=0}^{T-1}\|\nabla f(\theta_t)\|_{p^*}^{p^*}\right] \leq \frac{f(\theta_0)-f(\theta^*)}{\eta T} + \frac{1}{T}\sum_{t=0}^{T-1}\frac{\frac{2p-1}{p-1}G^{\frac{1}{p-1}}\|\vec{\sigma}\|_1}{\sqrt{n_t}} + \frac{L\eta G^{\frac{2}{p-1}}}{2}$$

where n_t is the batch size in iteration t and L, $\vec{\sigma}$, and G are constants from Assumption 1, 3, 4. Further letting the batch size $n_t = T$, the number of gradient call is $N = T^2$ for T iterations. With $\eta = \frac{1}{L^{\frac{1}{2}}G^{\frac{1}{p-1}}T^{\frac{1}{2}}}$ we have

$$\mathbb{E}\left[\frac{1}{T}\sum_{t=0}^{T-1}\|\nabla f(\theta_t)\|_{p^*}^{p^*}\right] \leq \frac{1}{N^{\frac{1}{4}}}\left[L^{\frac{1}{2}}G^{\frac{1}{p-1}}\left(f(\theta_0)-f(\theta^*)+\frac{1}{2}\right)+\frac{2p-1}{p-1}G^{\frac{1}{p-1}}\|\vec{\sigma}\|_1\right],$$

i.e., Algorithm 1 takes $N \in \mathcal{O}\left(\epsilon^{-4}\right)$ gradient queries to reach an ϵ-approximate stationary point.

Proof Sketch. Starting with Assumption 1 and the descent step in Algorithm 1,

$$f(\theta_{t+1}) \leq f(\theta_t) - \underbrace{\eta\left\langle \nabla f(\theta_t),\, s(\nabla f(\theta_t))\right\rangle}_{A} + \underbrace{\eta\left\langle \nabla f(\theta_t),\, s(\nabla f(\theta_t)) - s(g(\theta_t))\right\rangle}_{B} + \underbrace{\frac{L\eta^2}{2}\|s(g(\theta_t))\|_p^2}_{C},$$

where $A = \eta\|\nabla f(\theta_t)\|_{p^*}^{p^*}$. In conventional first-order analysis, the inner product term B is supposed to cancel out after taking expectation. In contrast, the closed-form stochastic ℓ_p descent update is coordinate-wise re-scaled, which makes the descent step *biased*, that is, $\mathbb{E}[s(g(x))] \neq s(f(x))$. In the literature on biased gradient descent (Stich & Ajalloeian, 2020; Demidovich et al., 2023), the bias terms simply accumulate as constants and do not decay with the iterations. Thus this term requires novel techniques to guarantee convergence. Noticing that $s_i(x) = \frac{x^{(i)}}{|x^{(i)}|^{\frac{p-2}{p-1}}} = \operatorname{sign}(x^{(i)})|x^{(i)}|^{\frac{1}{p-1}}$,

$$\begin{aligned}
B &= \eta\sum_{i=1}^{d}\nabla f(\theta_t)^{(i)}\left(\operatorname{sign}\left(\nabla f(\theta_t)^{(i)}\right)|\nabla f(\theta_t)^{(i)}|^{\frac{1}{p-1}} - \operatorname{sign}\left(g(\theta_t)^{(i)}\right)|g(\theta_t)^{(i)}|^{\frac{1}{p-1}}\right)\\
&= \eta\sum_{i=1}^{d}\left|\nabla f(\theta_t)^{(i)}\right|\left(|\nabla f(\theta_t)^{(i)}|^{\frac{1}{p-1}} + |g(\theta_t)^{(i)}|^{\frac{1}{p-1}}\right)\mathbb{I}\left[\operatorname{sign}\left(\nabla f(\theta_t)^{(i)}\right) \neq \operatorname{sign}\left(g(\theta_t)^{(i)}\right)\right]\\
&\quad + \eta\sum_{i=1}^{d}\left|\nabla f(\theta_t)^{(i)}\right|\left||\nabla f(\theta_t)^{(i)}|^{\frac{1}{p-1}} - |g(\theta_t)^{(i)}|^{\frac{1}{p-1}}\right|\mathbb{I}\left[\operatorname{sign}\left(\nabla f(\theta_t)^{(i)}\right) = \operatorname{sign}\left(g(\theta_t)^{(i)}\right)\right].
\end{aligned}$$

Denote the first term as B_1 and the second B_2. The $|\nabla f(\theta_t)^{(i)}|^{\frac{1}{p-1}} + |g(\theta_t)^{(i)}|^{\frac{1}{p-1}}$ term in B_1 can be bounded by $2G^{\frac{1}{p-1}}$ with Corollary 3, after which we take expectation, turning the indicator into a probability, and Lemma 2 in Appendix A.1 shows $\mathbb{E}\left[B_1\right] \leq \frac{2\eta G^{\frac{1}{p-1}}\|\vec{\sigma}\|_1}{\sqrt{n_t}}$ using Markov's inequality. B_2 requires more sophisticated handling since we cannot push the expectation through due to the data dependence of the term $\left||\nabla f(\theta_t)^{(i)}|^{\frac{1}{p-1}} - |g(\theta_t)^{(i)}|^{\frac{1}{p-1}}\right|$, nor does $\mathbb{P}\left[\operatorname{sign}\left(\nabla f(\theta_t)^{(i)}\right) = \operatorname{sign}\left(g(\theta_t)^{(i)}\right)\right]$ give us much information. We instead take the zeroth-order Taylor expansion so that $\forall\, i \in [d]$, $\exists\, \zeta^{(i)}$ between $\nabla f(\theta_t)^{(i)}$ and $g(\theta_t)^{(i)}$ such that

$$|\nabla f(\theta_t)^{(i)}|^{\frac{1}{p-1}} = |g(\theta_t)^{(i)}|^{\frac{1}{p-1}} + \frac{1}{p-1}\operatorname{sign}(\zeta^{(i)})\left|\zeta^{(i)}\right|^{\frac{2-p}{p-1}}\left(\nabla f(\theta_t)^{(i)} - g(\theta_t)^{(i)}\right)$$

And $\left||\nabla f(\theta_t)^{(i)}|^{\frac{1}{p-1}} - |g(\theta_t)^{(i)}|^{\frac{1}{p-1}}\right| = \frac{1}{p-1}\operatorname{sign}(\zeta^{(i)})\left|\zeta^{(i)}\right|^{\frac{2-p}{p-1}}\left(\nabla f(\theta_t)^{(i)} - g(\theta_t)^{(i)}\right)$. Furthermore, given $\operatorname{sign}\left(\nabla f(\theta_t)^{(i)}\right) = \operatorname{sign}\left(g(\theta_t)^{(i)}\right)$, it is either $\left|\nabla f(\theta_t)^{(i)}\right| \leq \left|\zeta^{(i)}\right| \leq \left|g(\theta_t)^{(i)}\right|$ or

Algorithm 2 STACEY$_{(p,2)}$ Optimizer

```
   input $p, \beta_1, \beta_2, \alpha, \tau, \eta, \epsilon, \lambda, f$
   initialize $\theta_0, z_0, m_0 \leftarrow 0$
1: while $\theta_{t+1}$ not converged do
2:     $g_t \leftarrow g(\theta_t)$                    $\triangleright\ g(\theta_t)$ s.t. $\mathbb{E}[g(\theta_t)] = \nabla f(\theta_t)$
3:     $c_{t+1} \leftarrow \beta_1 m_t + (1-\beta_1) g_t$
4:     $y_{t+1} \leftarrow \theta_t - \eta_t s_\epsilon(c_{t+1})$     $\triangleright\ s^\epsilon(x) = [s_1^\epsilon(x), \cdots, s_d^\epsilon(x)]^\top$ where $s_i^\epsilon(x) = \frac{x^{(i)}}{\left|x^{(i)}\right|^{\frac{p-2}{p-1}} + \epsilon}$
5:     $z_{t+1} = z_t - \alpha c_{t+1}$
6:     $\theta_{t+1} = \tau z_{t+1} + (1-\tau) y_{t+1} - \eta_t \lambda \theta_t$
7:     $m_{t+1} = \beta_2 m_t + (1-\beta_2) g_t$
   return $\theta_{t+1}$
```

$\left|\nabla f(\theta_t)^{(i)}\right| \geq \left|\zeta^{(i)}\right| \geq \left|g(\theta_t)^{(i)}\right|$. Appendix A.1 Lemma 3 shows that $\mathbb{E}\left[B_2\right] \leq \frac{\eta G^{\frac{1}{p-1}} \|\vec{\sigma}\|_1}{(p-1)\sqrt{n_t}}$ in either case.

Term C is usually turned into mean-squared error that coincides with variance in an unbiased setting, which the bounded variance assumption can directly handle. This is not the case for our setting. It is worth noting that the analysis of signSGD (Bernstein et al., 2018), a special case of the ℓ_p setting with $p = \infty$, was able to push through due to its update being in the very form of the sign of the gradient, which is in itself bounded by the constant 1. Our update, in contrast, is much more complicated with the absolute value of the coordinates of the gradient in the denominator, which is only lower bounded 0, or some $\epsilon > 0$ at best. Therefore, we directly apply Assumption 4 and $C = \frac{L\eta^2}{2}\|\nabla f(\theta_t)\|_{p^*}^{\frac{2}{p-1}} \leq \frac{L\eta^2 G^{\frac{2}{p-1}}}{2}$. Moving term A to the left hand side, telescoping through iteration 0 to $T-1$, and dividing both sides by ηT completes the proof. □

4 ACCELERATING STOCHASTIC STEEPEST DESCENT

Building on the *unaccelerated* stochastic ℓ_p descent for non-convex settings, we present accelerated versions of the method through the interpolation of two sequences in primal and dual spaces. Indeed, this type of interpolation is the basis of the linear coupling framework (Allen-Zhu & Orecchia, 2017), wherein a steepest descent step is carefully coupled with a mirror descent step. Similar "coupling" can also be found in Nesterov's generalization of standard AGD to non-Euclidean settings (Nesterov, 2005) and recent acceleration for ℓ_p descent in the deterministic convex setting (Bai & Bullins, 2024). Inspired by these previous examples (and their successes, e.g., (Bullins, 2020; Jambulapati et al., 2019; Sherman, 2017; Sidford & Tian, 2018)), we introduce a practical acceleration scheme called STACEY, which is *specifically designed for non-Euclidean methods*. As presented in Algorithm 2, the algorithm takes the steepest descent step with respect to the ℓ_p-norm in line 4 and then a gradient step in line 5. The update on the variable θ is an interpolation between the two, controlled by the parameter τ. The algorithm generalizes linear coupling (Allen-Zhu & Orecchia, 2017) with non-Euclidean steepest descent while taking the mirror descent step with the distance generating function chosen as $\frac{1}{2}\|\cdot\|_2^2$. We further specify the name as STACEY$_{(p,2)}$ to clarify the norms in which the steepest descent and mirror descent steps are taken.

We wish to note that even though for smooth convex optimization, (deterministic) gradient descent can be accelerated to achieve a rate of $O(1/T^2)$, for stochastic first-order methods, however, it has been shown that a) in convex settings, SGD cannot improve upon the standard $O(1/\sqrt{T})$ rate when noise parameter σ is large enough (Agarwal et al., 2009), and b) in first-order smooth *non-convex* settings, *SGD cannot be accelerated (in theory)* without additional assumptions (in terms of gradient norm minimization), due to known lower bounds (Arjevani et al., 2023). Nevertheless, standard practical implementations of SGD are frequently designed to introduce *some* notion of acceleration with momentum (e.g., (Bernstein et al., 2018; Sutskever et al., 2013)),[7] "pushing" the converging sequence further along the direction of previous gradients.

[7] Momentum coincides with Nesterov's acceleration in the deterministic convex setting, though this by no means makes them equivalent in stochastic non-convex settings.

Algorithm 3 $\textsc{Stacey}_{(p,p)}$ Optimizer

```
    input $p, \beta_1, \beta_2, \alpha, \tau, \eta, \epsilon, \lambda, f$
    initialize $\theta_0, z_0, m_0 \leftarrow 0$
1: while $\theta_{t+1}$ not converged do
2:     $g_t \leftarrow g(\theta_t)$                ▷ $g(\theta_t)$ s.t. $\mathbb{E}[g(\theta_t)] = \nabla f(\theta_t)$
3:     $c_{t+1} \leftarrow \beta_1 m_t + (1-\beta_1) g_t$
4:     $y_{t+1} \leftarrow \theta_t - \eta_t s_\epsilon(c_{t+1})$    ▷ $s^\epsilon(x) = [s_1^\epsilon(x), \cdots, s_d^\epsilon(x)]^\top$ where $s_i^\epsilon(x) = \frac{x^{(i)}}{|x^{(i)}|^{\frac{p-2}{p-1}} + \epsilon}$
5:     $z_{t+1}^{(i)} = \frac{|z_t^{(i)}|^{p-2} z_t^{(i)} - \alpha c_{t+1}^{(i)}}{\left| |z_t^{(i)}|^{p-2} z_t^{(i)} - \alpha c_{t+1}^{(i)} \right|^{\frac{p-2}{p-1}}}, \forall\, i \in [d]$
6:     $\theta_{t+1} = \tau z_{t+1} + (1-\tau) y_{t+1} - \eta_t \lambda \theta_t$
7:     $m_{t+1} = \beta_2 m_t + (1-\beta_2) g_t$
    return $\theta_{t+1}$
```

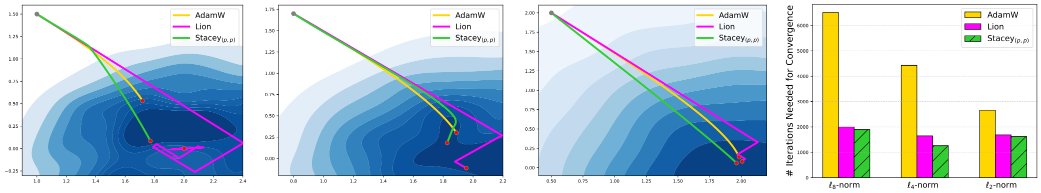

(a) $\mathcal{N}_8$ distribution (b) $\mathcal{N}_4$ distribution (c) $\mathcal{N}_2$ distribution (d) Convergence speed

Figure 1: Results on synthetic p-generalized Gaussian distributions. Stacey optimizer is more stable on highly non-Euclidean distributions, and converges faster than AdamW and Lion.

In contrast, we take the view of acceleration not as a "pushing" (in the Euclidean sense), but rather as a (dynamic) interpolation of two iterate sequences: one acting from a (primal) steepest descent perspective (line 4 Algorithm 2), while the other functions in a dual capacity (line 5 Algorithm 2). An obvious distinction (pun intended) is momentum, as a separate functionality, can be applied on top of the acceleration scheme in $\textsc{Stacey}_{(p,2)}$, as demonstrated in lines 3 and 7 of Algorithm 2, for both the steepest descent and the gradient descent.

In the realm of non-Euclidean methods, we contrast our algorithm with Lion-$\mathcal{K}$ (Chen et al., 2024; Bernstein et al., 2018). While at first glance it may seem that these methods may simply be a rewriting of each other (based on the choice of parameters), a closer inspection on *the very first step* reveals that such is not the case:

$$\begin{aligned} \text{Lion-}\mathcal{K}\text{: } \theta_1 &= -\eta \nabla \mathcal{K}\left((1-\beta_1) g(\theta_0)\right), \\ \textsc{Stacey}_{(p,2)}\text{: } \theta_1 &= -(1-\tau)\eta s^\epsilon\left((1-\beta_1) g(\theta_0)\right) - \tau\alpha(1-\beta_1) g(\theta_0). \end{aligned}$$

where $\mathcal{K}(\cdot) = \|\cdot\|_p$ and $s^\epsilon(\cdot)$ is defined in Algorithm 2. The key difference of $\textsc{Stacey}_{(p,2)}$ lies in the convex combination of a steepest descent step and a gradient descent step, whereas Lion-$\mathcal{K}$ is composed of only the steepest descent step. They only coincide when $\tau = 0$ for $\textsc{Stacey}_{(p,2)}$, i.e., completely getting rid of the "coupling", which then defeats the purpose of our acceleration. In addition, there is no choice of parameters for Lion-$\mathcal{K}$ to recover linear coupling. As a result, they are not iterate-equivalent, which further highlights the fundamental difference between "momentum" and "acceleration", a distinction which, crucially, does not appear in the case of standard (Euclidean) AGD, i.e., when both steepest and mirror descent steps are with respect to Euclidean norms.

Further inspired by the fact that $\textsc{Stacey}_{(p,2)}$ breaks the symmetry (in primal and dual trajectories) by coupling an ℓ_p steepest descent step with an ℓ_2-based mirror descent step, we present the natural variant $\textsc{Stacey}_{(p,p)}$ (Algorithm 3), for which we group ℓ_p steepest descent with a mirror descent step having $\frac{1}{p}\|\cdot\|_p^p$ (whose p^{th}-order uniform convexity is useful for non-Euclidean acceleration (Song et al., 2019)) as its distance generating function. The closed-form mirror descent update is presented in line 5 of the algorithms.

Table 1: Image classification on CIFAR at the 50th, 100th, and 200th epochs. STACEY consistently outperforms other optimizers at all epochs, demonstrating both superior accuracy and faster convergence.

Optimizer	Training NLL ↓			Testing ACC (%) ↑		
	@50 epoch	@100 epoch	@200 epoch	@50 epoch	@100 epoch	@200 epoch
SGD w/ Nesterov	0.0523	0.0342	0.0289	91.78	91.93	92.69
Adam	0.1303	0.0487	0.0229	90.03	90.63	91.58
AdamW	0.0620	0.0298	0.0170	89.99	91.39	91.89
Lion	0.0410	0.0199	0.0103	91.85	92.48	92.69
STACEY$_{(p,p)}$	0.1438	0.0405	0.0006	88.95	91.50	**94.05**
STACEY$_{(p,2)}$	**0.0375**	**0.0104**	**0.0005**	**91.87**	**92.92**	93.99

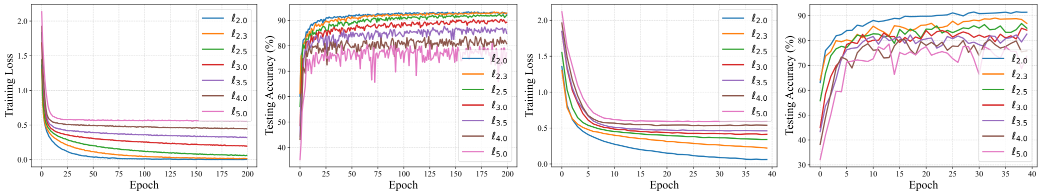

(a) Training loss curves of STACEY$_{(p,p)}$ (b) Testing ACC curves of STACEY$_{(p,p)}$ (c) Training loss curves of STACEY$_{(p,2)}$ (d) Testing ACC curves of STACEY$_{(p,2)}$

Figure 2: Learning curves of CIFAR classification with varying ℓ_p-norm.

5 EXPERIMENTS

In this section, we present empirical evidence that the STACEY optimizer outperforms other optimizers in both convergence speed and accuracy. We evaluate STACEY's effectiveness on synthetic distributions (Section 5.1), image classification (Section 5.2), and LLM pretraining (Section 5.3). The hyperparameter choices are summarized in Appendix D.

In all experiments, we underscore the efficiency of the STACEY optimizer by comparing it against other optimizers as baselines including SGD (with Nesterov's momentum) (Nesterov, 1983), Adam (Kingma, 2014), AdamW (Loshchilov & Hutter, 2019), and Lion (Chen et al., 2023). For synthetic distribution estimation, we demonstrate that STACEY outperforms Lion and AdamW in convergence speed on generated ℓ_p Gaussian datasets.

In real-world large datasets, such as training from scratch on ImageNet (Deng et al., 2009) and LLM (LLaMA (Touvron et al., 2023)) pretraining on C4, we further demonstrate the necessity of utilizing different ℓ_p-norms for specific tasks. For example, in the CIFAR image classification, an ℓ_p-norm for p close to 2 delivers the best performance (Section 5.2), consistent with the effectiveness of Euclidean-based optimizers. In contrast, a ℓ_p-norm with p around 3 proves more effective in LLM pertaining (Section 5.3). These results highlight the importance of developing non-Euclidean optimizers and adjusting the choice of ℓ_p-norm to enhance performance across different tasks.

5.1 ESTIMATING SYNTHETIC DISTRIBUTIONS

STACEY optimizer is designed for generalized ℓ_p-norm optimization with $p \geq 2$. Following D'Angelo & Fortuin (2021); Li & Zhang (2024), we visualize the trajectory of optimizers when estimating synthetic distributions in Fig. 1, to demonstrate STACEY's faster convergence compared to other optimizers on p-generalized Gaussian distributions (Subbotin, 1923; Kalke & Richter, 2013). The synthetic distributions $\mathcal{N}_p(\boldsymbol{\mu})$ marginally follow the p-generalized Gaussian distribution whose *probability density function* (PDF) is given by $p\left(\mathbf{x}^{(i)}\right) = \frac{p^{1-1/p}}{2\Gamma(1/p)} \exp\left\{-\left|\boldsymbol{x}^{(i)} - \boldsymbol{\mu}^{(i)}\right|^p / p\right\}$, and thus the PDF of $\mathcal{N}_p(\boldsymbol{\mu})$ is

$$p(\boldsymbol{x}) = \prod_{i=1}^{d} p\left(\mathbf{x}^{(i)}\right) \propto \exp\left\{-\sum_{i=1}^{d} \frac{\left|\boldsymbol{x}^{(i)} - \boldsymbol{\mu}^{(i)}\right|^p}{p}\right\} = \exp\left\{-\frac{\|\boldsymbol{x} - \boldsymbol{\mu}\|_p^p}{p}\right\}.$$

Table 2: Image classification on ImageNet at the 20th, 50th, and 90th epochs. STACEY consistently outperforms other optimizers at all epochs, demonstrating both superior accuracy and faster convergence.

Optimizer	Training NLL ↓			Testing Top-1 ACC (%) ↑		
	@20 epoch	@50 epoch	@90 epoch	@20 epoch	@50 epoch	@90 epoch
SGD	3.9729	2.4376	1.9257	21.05	45.94	63.17
STACEY$_{(p,p)}$	**1.9371**	**1.2064**	**0.9902**	**60.84**	**68.23**	**69.88**
STACEY$_{(p,2)}$	3.3706	2.5149	2.1975	32.16	49.39	57.33

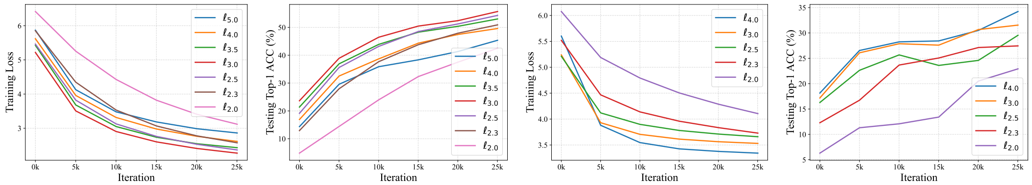

(a) Training loss curves of STACEY$_{(p,p)}$ (b) Testing ACC curves of STACEY$_{(p,p)}$ (c) Training loss curves of STACEY$_{(p,2)}$ (d) Testing ACC curves of STACEY$_{(p,2)}$

Figure 3: Learning curves of ImageNet classification at the first 6 epochs with varying ℓ_p-norm.

We sample synthetic datasets from $\mathcal{N}_p([2,0]^T)$ distributions with varying p values, where larger p typically yields more complex non-Euclidean optimization problems. For each optimizer, we set their learning rates to be 10^{-3} and plot 5000-iteration trajectories. Results show that STACEY maintains stable convergence even with larger p values. In contrast, AdamW (Loshchilov & Hutter, 2019) converges more slowly, and Lion (Chen et al., 2023) exhibits significant fluctuations.

Fig. 1d compares the average convergence rates of different optimizers. We initialize points from a standard Gaussian distribution and repeat each experiment 100 times. Results show that STACEY converges faster than AdamW and Lion, especially on the highly non-Euclidean $\mathcal{N}_8$ distribution.

5.2 IMAGE CLASSIFICATION

We demonstrate improved accuracy and faster convergence of the STACEY optimizer across image classification tasks of varying scales, consistent with our algorithm's design for acceleration.

Training from scratch on CIFAR. We train ResNet18 (He et al., 2016) on the CIFAR dataset (Krizhevsky, 2009) for 200 epochs, with the results presented in Table 1. We report training NLL and testing accuracy at the 50th, 100th, and 200th epochs. The proposed STACEY optimizer consistently outperforms all compared optimizers. As shown in Fig. 2, a p-norm of 2 yields the best performance for the CIFAR dataset when using the ResNet18 architecture.

Training from scratch on ImageNet. We train ResNet50 (He et al., 2016) with a batch size 256[8] on ImageNet (Deng et al., 2009) for 90 epochs. The learning rate schedule is cosine with 10K steps warm up, and the momentum is saved as `bfloat16` to reduce the memory footprint. The learning curves are shown in Table 2.

5.3 PRETRAINING LARGE LANGUAGE MODELS (LLMS)

We pretrain LLaMA 100M (Touvron et al., 2023) on the C4 dataset[9] using various optimizers. The learning curves, presented in Fig.4, show that the STACEY optimizer outperforms the alternatives. Additionally, Fig.5 indicates that a p-norm of 3 yields the best performance, which contrasts with the optimal $p = 2$ observed in the CIFAR image classification tasks discussed in Section 5.2.

[8] Our batch size 256 is significantly smaller than Lion's (Chen et al., 2024) batch size 1024.

[9] `https://huggingface.co/datasets/allenai/c4`.

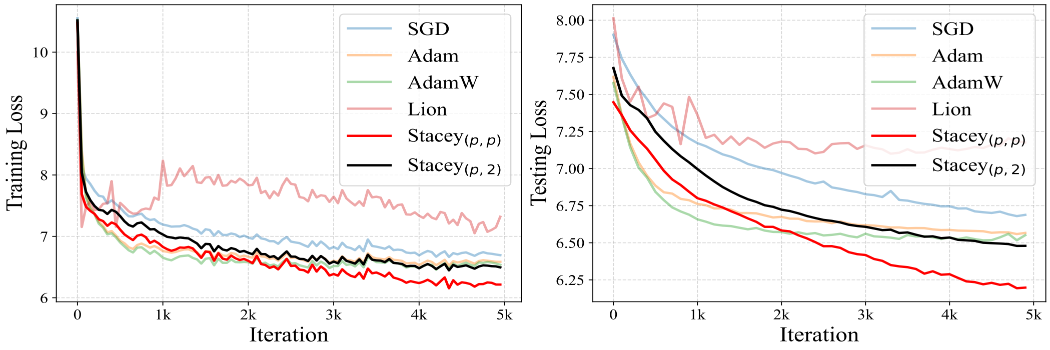

(a) Training loss curves

(b) Testing ACC curves

Figure 4: Learning curves of LLM pretraining at the first 5000 iterations among different optimizers.

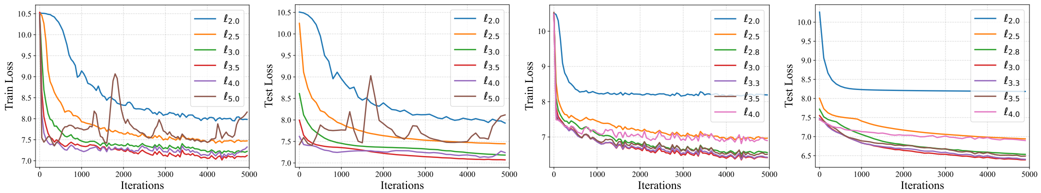

(a) Training loss curves of STACEY$_{(p,p)}$

(b) Testing loss curves of STACEY$_{(p,p)}$

(c) Training loss curves of STACEY$_{(p,2)}$

(d) Testing loss curves of STACEY$_{(p,2)}$

Figure 5: Learning curves of LLM pretraining at the first 5000 iterations with varying ℓ_p-norm.

5.4 DISCUSSION

As we observe throughout the experiments, STACEY demonstrates superior performance over SGD, which showcases its ability to adapt to a broader range of non-Euclidean geometries. This adaptability verifies STACEY's convergence for general ℓ_p-norms, making it a better choice for optimization tasks that present complex geometries and extend beyond the conventional Euclidean frameworks. Compared with Adam and AdamW, STACEY confirms that the introduced acceleration technique is well-aligned with the principles of non-Euclidean optimization. The superior results validate that STACEY's acceleration mechanism, which is purposefully designed for non-Euclidean spaces, outperforms the traditional adaptive methods that rely on Euclidean-centric assumptions. Furthermore, STACEY's improved performance over Lion highlights the effectiveness of interpolating primal and dual sequences as an acceleration strategy, in contrast to simply incorporating momentum. The primal-dual interpolation ensures a more balanced and stable progression towards optimality, leveraging information from both primal and dual sequences. This strategy allows STACEY to achieve faster convergence, even in challenging settings and complex tasks like large-scale image classification and pretraining LLMs.

6 CONCLUSION

This paper investigates the steepest descent algorithm in ℓ_p norm for stochastic non-convex optimization. We establish for the stochastic ℓ_p descent algorithm an $O(\epsilon^{-4})$ convergence rate in expectation to a stationary point with respect to the dual norm $\|\cdot\|_{p^*}^{p^*}$. Building on these techniques, we further proposed an acceleration scheme for non-Euclidean methods, incorporated stochastic ℓ_p descent with mirror descent, and presented an accelerated algorithm called STACEY. We evaluated the performance of STACEY on large-scale image classification and pretraining language modeling tasks and achieved both faster convergence and higher accuracy compared to other methods.

Reproducibility Statement

The reproducibility of our research is ensured through two key measures. Firstly, the algorithm proposed in this paper has been explicitly described in detail in the appendix, allowing for a clear understanding of our approach. Secondly, to facilitate direct replication of our work, we have provided the complete implementations as anonymously downloadable source code in the supplementary materials. These measures should enable other researchers to fully reproduce and validate our findings.

References

Leonard Adolphs, Jonas Kohler, and Aurelien Lucchi. Ellipsoidal trust region methods and the marginal value of hessian information for neural network training. *arXiv preprint arXiv:1905.09201*, 2019. (Cited on page 2.)

Alekh Agarwal, Martin J Wainwright, Peter Bartlett, and Pradeep Ravikumar. Information-theoretic lower bounds on the oracle complexity of convex optimization. *Advances in Neural Information Processing Systems*, 22, 2009. (Cited on page 6.)

Naman Agarwal, Zeyuan Allen-Zhu, Brian Bullins, Elad Hazan, and Tengyu Ma. Finding approximate local minima faster than gradient descent. In *Proceedings of the 49th Annual ACM SIGACT Symposium on Theory of Computing*, pp. 1195–1199, 2017. (Cited on page 1.)

Naman Agarwal, Brian Bullins, Xinyi Chen, Elad Hazan, Karan Singh, Cyril Zhang, and Yi Zhang. Efficient full-matrix adaptive regularization. In *International Conference on Machine Learning*, pp. 102–110. PMLR, 2019. (Cited on page 3.)

Zeyuan Allen-Zhu and Lorenzo Orecchia. Linear coupling: An ultimate unification of gradient and mirror descent. In *8th Innovations in Theoretical Computer Science Conference (ITCS 2017)*. Schloss Dagstuhl-Leibniz-Zentrum fuer Informatik, 2017. (Cited on pages 2, 3, and 6.)

Zeyuan Allen-Zhu, Yuanzhi Li, and Yingyu Liang. Learning and generalization in overparameterized neural networks, going beyond two layers. *Advances in neural information processing systems*, 32, 2019a. (Cited on page 1.)

Zeyuan Allen-Zhu, Yuanzhi Li, and Zhao Song. A convergence theory for deep learning via over-parameterization. In *International conference on machine learning*, pp. 242–252. PMLR, 2019b. (Cited on page 1.)

Yossi Arjevani, Yair Carmon, John C Duchi, Dylan J Foster, Nathan Srebro, and Blake Woodworth. Lower bounds for non-convex stochastic optimization. *Mathematical Programming*, 199(1):165–214, 2023. (Cited on pages 3 and 6.)

Sanjeev Arora, Simon Du, Wei Hu, Zhiyuan Li, and Ruosong Wang. Fine-grained analysis of optimization and generalization for overparameterized two-layer neural networks. In *International Conference on Machine Learning*, pp. 322–332. PMLR, 2019a. (Cited on page 1.)

Sanjeev Arora, Simon S Du, Wei Hu, Zhiyuan Li, Russ R Salakhutdinov, and Ruosong Wang. On exact computation with an infinitely wide neural net. *Advances in neural information processing systems*, 32, 2019b. (Cited on page 1.)

Site Bai and Brian Bullins. Faster acceleration for steepest descent. *arXiv preprint arXiv:2409.19200*, 2024. (Cited on pages 2, 4, and 6.)

Lukas Balles, Fabian Pedregosa, and Nicolas Le Roux. The geometry of sign gradient descent. *arXiv preprint arXiv:2002.08056*, 2020. (Cited on pages 1, 2, 4, and 19.)

Sue Becker, Yann Le Cun, et al. Improving the convergence of back-propagation learning with second order methods. In *Proceedings of the 1988 connectionist models summer school*, pp. 29–37, 1988. (Cited on page 2.)

Jeremy Bernstein, Yu-Xiang Wang, Kamyar Azizzadenesheli, and Animashree Anandkumar. signsgd: Compressed optimisation for non-convex problems. In *International Conference on Machine Learning*, pp. 560–569. PMLR, 2018. (Cited on pages 1, 2, 4, 6, 7, and 19.)

Stephen Boyd and Lieven Vandenberghe. *Convex optimization*. Cambridge university press, 2004. (Cited on page 3.)

Sébastien Bubeck et al. Convex optimization: Algorithms and complexity. *Foundations and Trends® in Machine Learning*, 8(3-4):231–357, 2015. (Cited on pages 2 and 3.)

Brian Bullins. Highly smooth minimization of non-smooth problems. In *Conference on Learning Theory*, pp. 988–1030. PMLR, 2020. (Cited on page 6.)

David Carlson, Ya-Ping Hsieh, Edo Collins, Lawrence Carin, and Volkan Cevher. Stochastic spectral descent for discrete graphical models. *IEEE Journal of Selected Topics in Signal Processing*, 10(2):296–311, 2015. (Cited on page 2.)

Yair Carmon, John C Duchi, Oliver Hinder, and Aaron Sidford. "convex until proven guilty": dimension-free acceleration of gradient descent on non-convex functions. In *International conference on machine learning*, pp. 654–663. PMLR, 2017. (Cited on page 1.)

Yair Carmon, John C Duchi, Oliver Hinder, and Aaron Sidford. Accelerated methods for nonconvex optimization. *SIAM Journal on Optimization*, 28(2):1751–1772, 2018. (Cited on page 1.)

Yair Carmon, John C Duchi, Oliver Hinder, and Aaron Sidford. Lower bounds for finding stationary points i. *Mathematical Programming*, 184(1):71–120, 2020. (Cited on page 3.)

Yair Carmon, John C Duchi, Oliver Hinder, and Aaron Sidford. Lower bounds for finding stationary points ii: first-order methods. *Mathematical Programming*, 185(1):315–355, 2021. (Cited on page 3.)

Lizhang Chen, Bo Liu, Kaizhao Liang, et al. Lion secretly solves a constrained optimization: As lyapunov predicts. In *The Twelfth International Conference on Learning Representations*, 2024. (Cited on pages 1, 7, and 9.)

Xiangning Chen, Chen Liang, Da Huang, Esteban Real, Kaiyuan Wang, Hieu Pham, Xuanyi Dong, Thang Luong, Cho-Jui Hsieh, Yifeng Lu, et al. Symbolic discovery of optimization algorithms. *Advances in neural information processing systems*, 36, 2023. (Cited on pages 1, 8, and 9.)

Jeremy Cohen, Simran Kaur, Yuanzhi Li, J Zico Kolter, and Ameet Talwalkar. Gradient descent on neural networks typically occurs at the edge of stability. In *International Conference on Learning Representations*, 2021a. (Cited on page 2.)

Michael B Cohen, Aaron Sidford, and Kevin Tian. Relative lipschitzness in extragradient methods and a direct recipe for acceleration. In *12th Innovations in Theoretical Computer Science Conference (ITCS 2021)*. Schloss Dagstuhl-Leibniz-Zentrum für Informatik, 2021b. (Cited on page 2.)

Francesco D'Angelo and Vincent Fortuin. Repulsive deep ensembles are bayesian. *Advances in Neural Information Processing Systems*, 34:3451–3465, 2021. (Cited on page 8.)

Yury Demidovich, Grigory Malinovsky, Igor Sokolov, and Peter Richtárik. A guide through the zoo of biased SGD. In *Thirty-seventh Conference on Neural Information Processing Systems*, 2023. URL `https://openreview.net/forum?id=OCtv4NyahI`. (Cited on page 5.)

Jia Deng, Wei Dong, Richard Socher, Li-Jia Li, Kai Li, and Li Fei-Fei. Imagenet: A large-scale hierarchical image database. In *2009 IEEE conference on computer vision and pattern recognition*, pp. 248–255. Ieee, 2009. (Cited on pages 8, 9, and 20.)

Jelena Diakonikolas and Cristóbal Guzmán. Complementary composite minimization, small gradients in general norms, and applications. *Mathematical Programming*, pp. 1–45, 2024. (Cited on pages 2 and 3.)

Timothy Dozat. Incorporating nesterov momentum into. In *Proceedings of the 4th International Conference on Learning Representations*, pp. 1–4, 2016. (Cited on page 3.)

Simon Du, Jason Lee, Haochuan Li, Liwei Wang, and Xiyu Zhai. Gradient descent finds global minima of deep neural networks. In *International Conference on Machine Learning*, pp. 1675–1685. PMLR, 2019. (Cited on page 1.)

Simon S Du, Chi Jin, Jason D Lee, Michael I Jordan, Aarti Singh, and Barnabas Poczos. Gradient descent can take exponential time to escape saddle points. *Advances in Neural Information Processing Systems*, 30, 2017. (Cited on page 1.)

Simon S Du, Xiyu Zhai, Barnabas Poczos, and Aarti Singh. Gradient descent provably optimizes over-parameterized neural networks. In *International Conference on Learning Representations*, 2018. (Cited on page 1.)

John Duchi, Elad Hazan, and Yoram Singer. Adaptive subgradient methods for online learning and stochastic optimization. *Journal of machine learning research*, 12(7), 2011. (Cited on pages 1 and 3.)

Rong Ge, Furong Huang, Chi Jin, and Yang Yuan. Escaping from saddle points—online stochastic gradient for tensor decomposition. In *Conference on learning theory*, pp. 797–842. PMLR, 2015. (Cited on page 1.)

Saeed Ghadimi and Guanghui Lan. Stochastic first-and zeroth-order methods for nonconvex stochastic programming. *SIAM journal on optimization*, 23(4):2341–2368, 2013. (Cited on pages 1 and 2.)

Behrooz Ghorbani, Shankar Krishnan, and Ying Xiao. An investigation into neural net optimization via hessian eigenvalue density. In *International Conference on Machine Learning*, pp. 2232–2241. PMLR, 2019. (Cited on page 2.)

Suriya Gunasekar, Jason Lee, Daniel Soudry, and Nathan Srebro. Characterizing implicit bias in terms of optimization geometry. In *International Conference on Machine Learning*, pp. 1832–1841. PMLR, 2018a. (Cited on page 1.)

Suriya Gunasekar, Jason D Lee, Daniel Soudry, and Nati Srebro. Implicit bias of gradient descent on linear convolutional networks. *Advances in neural information processing systems*, 31, 2018b. (Cited on page 1.)

Vineet Gupta, Tomer Koren, and Yoram Singer. Shampoo: Preconditioned stochastic tensor optimization. In *International Conference on Machine Learning*, pp. 1842–1850. PMLR, 2018. (Cited on page 3.)

Cristóbal Guzmán and Arkadi Nemirovski. On lower complexity bounds for large-scale smooth convex optimization. *Journal of Complexity*, 31(1):1–14, 2015. (Cited on pages 2 and 3.)

Kaiming He, Xiangyu Zhang, Shaoqing Ren, and Jian Sun. Deep residual learning for image recognition. In *Proceedings of the IEEE conference on computer vision and pattern recognition*, pp. 770–778, 2016. (Cited on page 9.)

Arthur Jacot, Franck Gabriel, and Clément Hongler. Neural tangent kernel: Convergence and generalization in neural networks. *Advances in neural information processing systems*, 31, 2018. (Cited on page 1.)

Arun Jambulapati, Aaron Sidford, and Kevin Tian. A direct tilde {O}(1/epsilon) iteration parallel algorithm for optimal transport. *Advances in Neural Information Processing Systems*, 32, 2019. (Cited on page 6.)

Kaiqi Jiang, Dhruv Malik, and Yuanzhi Li. How does adaptive optimization impact local neural network geometry? *Advances in Neural Information Processing Systems*, 36, 2024. (Cited on page 2.)

Chi Jin, Rong Ge, Praneeth Netrapalli, Sham M Kakade, and Michael I Jordan. How to escape saddle points efficiently. In *International conference on machine learning*, pp. 1724–1732. PMLR, 2017. (Cited on page 1.)

Steve Kalke and W-D Richter. Simulation of the p-generalized gaussian distribution. *Journal of Statistical Computation and Simulation*, 83(4):641–667, 2013. (Cited on page 8.)

Hamed Karimi, Julie Nutini, and Mark Schmidt. Linear convergence of gradient and proximal-gradient methods under the polyak-łojasiewicz condition. In *Machine Learning and Knowledge Discovery in Databases: European Conference, ECML PKDD 2016, Riva del Garda, Italy, September 19-23, 2016, Proceedings, Part I 16*, pp. 795–811. Springer, 2016. (Cited on page 19.)

Jonathan A Kelner, Yin Tat Lee, Lorenzo Orecchia, and Aaron Sidford. An almost-linear-time algorithm for approximate max flow in undirected graphs, and its multicommodity generalizations. In *Proceedings of the twenty-fifth annual ACM-SIAM symposium on Discrete algorithms*, pp. 217–226. SIAM, 2014. (Cited on pages 2 and 3.)

Diederik P Kingma. Adam: A method for stochastic optimization. *arXiv preprint arXiv:1412.6980*, 2014. (Cited on pages 1, 3, and 8.)

A Krizhevsky. Learning multiple layers of features from tiny images. *Master's thesis, University of Tront*, 2009. (Cited on pages 9 and 20.)

Bolian Li and Ruqi Zhang. Entropy-mcmc: Sampling from flat basins with ease. In *The Twelfth International Conference on Learning Representations*, 2024. (Cited on pages 2 and 8.)

Xinyan Li, Qilong Gu, Yingxue Zhou, Tiancong Chen, and Arindam Banerjee. Hessian based analysis of sgd for deep nets: Dynamics and generalization. In *Proceedings of the 2020 SIAM International Conference on Data Mining*, pp. 190–198. SIAM, 2020. (Cited on page 2.)

Hong Liu, Zhiyuan Li, David Leo Wright Hall, Percy Liang, and Tengyu Ma. Sophia: A scalable stochastic second-order optimizer for language model pre-training. In *International Conference on Learning Representations*, 2024. (Cited on page 3.)

Liyuan Liu, Haoming Jiang, Pengcheng He, Weizhu Chen, Xiaodong Liu, Jianfeng Gao, and Jiawei Han. On the variance of the adaptive learning rate and beyond. In *International Conference on Learning Representations*, 2020. (Cited on page 3.)

Ilya Loshchilov and Frank Hutter. Decoupled weight decay regularization. In *International Conference on Learning Representations*, 2019. (Cited on pages 1, 8, and 9.)

Arkaddii S Nemirovskii and Yu E Nesterov. Optimal methods of smooth convex minimization. *(In Russian). USSR Computational Mathematics and Mathematical Physics*, 25(2):21–30, 1985. (Cited on pages 2 and 3.)

Arkadij Semenovič Nemirovskij and David Borisovich Yudin. Problem complexity and method efficiency in optimization. 1983. (Cited on page 3.)

Yu Nesterov. Smooth minimization of non-smooth functions. *Mathematical programming*, 103:127–152, 2005. (Cited on pages 2, 3, and 6.)

Yurii Nesterov. A method for solving the convex programming problem with convergence rate o (1/k2). In *Dokl akad nauk Sssr*, volume 269, pp. 543, 1983. (Cited on pages 1, 2, 3, and 8.)

Yurii Nesterov. *Lectures on convex optimization*, volume 137. Springer, 2018. (Cited on page 2.)

Vardan Papyan. The full spectrum of deepnet hessians at scale: Dynamics with sgd training and sample size. *arXiv preprint arXiv:1811.07062*, 2018. (Cited on page 2.)

Boris T Polyak. Some methods of speeding up the convergence of iteration methods. *Ussr computational mathematics and mathematical physics*, 4(5):1–17, 1964. (Cited on pages 1 and 3.)

Sashank J Reddi, Satyen Kale, and Sanjiv Kumar. On the convergence of adam and beyond. In *International Conference on Learning Representations*, 2018. (Cited on page 3.)

Martin Riedmiller and Heinrich Braun. Rprop: a fast adaptive learning algorithm. In *Proc. of the Int. Symposium on Computer and Information Science VII*, 1992. (Cited on page 1.)

Herbert Robbins and Sutton Monro. A stochastic approximation method. *The annals of mathematical statistics*, pp. 400–407, 1951. (Cited on pages 1 and 3.)

Jonah Sherman. Area-convexity, ℓ_∞ regularization, and undirected multicommodity flow. In *Proceedings of the 49th Annual ACM SIGACT Symposium on Theory of Computing*, pp. 452–460, 2017. (Cited on pages 2 and 6.)

Aaron Sidford and Kevin Tian. Coordinate methods for accelerating ℓ_∞ regression and faster approximate maximum flow. In *2018 IEEE 59th Annual Symposium on Foundations of Computer Science (FOCS)*, pp. 922–933. IEEE, 2018. (Cited on pages 2 and 6.)

Chaobing Song, Yong Jiang, and Yi Ma. Unified acceleration of high-order algorithms under h\"{o} lder continuity and uniform convexity. *arXiv preprint arXiv:1906.00582*, 2019. (Cited on pages 3 and 7.)

Daniel Soudry, Elad Hoffer, Mor Shpigel Nacson, Suriya Gunasekar, and Nathan Srebro. The implicit bias of gradient descent on separable data. *Journal of Machine Learning Research*, 19(70):1–57, 2018. (Cited on page 1.)

Sebastian U Stich and Ahmad Ajalloeian. Analysis of sgd with biased gradient estimators. *arXiv preprint arXiv:2008.00051*, 2020. (Cited on page 5.)

M. T. Subbotin. On the law of frequency of error. *Mat. Sb.*, 31:296–301, 1923. URL `http://mi.mathnet.ru/sm6854`. (Cited on page 8.)

Ilya Sutskever, James Martens, George Dahl, and Geoffrey Hinton. On the importance of initialization and momentum in deep learning. In *International conference on machine learning*, pp. 1139–1147. PMLR, 2013. (Cited on pages 3 and 6.)

Hugo Touvron, Thibaut Lavril, Gautier Izacard, Xavier Martinet, Marie-Anne Lachaux, Timothée Lacroix, Baptiste Rozière, Naman Goyal, Eric Hambro, Faisal Azhar, et al. Llama: Open and efficient foundation language models. *arXiv preprint arXiv:2302.13971*, 2023. (Cited on pages 8 and 9.)

Rachel Ward, Xiaoxia Wu, and Leon Bottou. Adagrad stepsizes: Sharp convergence over nonconvex landscapes. *Journal of Machine Learning Research*, 21(219):1–30, 2020. (Cited on page 1.)

Ashia C Wilson, Rebecca Roelofs, Mitchell Stern, Nati Srebro, and Benjamin Recht. The marginal value of adaptive gradient methods in machine learning. *Advances in Neural Information Processing Systems*, 30, 2017. (Cited on page 1.)

Matthew D Zeiler. Adadelta: an adaptive learning rate method. *arXiv preprint arXiv:1212.5701*, 2012. (Cited on page 3.)

A Proofs

A.1 Complete Proof for Theorem 1

Theorem 1 (Main). *Running Algorithm 1 on some (possibly non-convex) function f that satisfies Assumptions 1 to 4 yields*

$$\mathbb{E}\left[\frac{1}{T}\sum_{t=0}^{T-1}\|\nabla f(\theta_t)\|_{p^*}^{p^*}\right] \leq \frac{f(\theta_0)-f(\theta^*)}{\eta T} + \frac{1}{T}\sum_{t=0}^{T-1}\frac{\frac{2p-1}{p-1}G^{\frac{1}{p-1}}\|\vec{\sigma}\|_1}{\sqrt{n_t}} + \frac{L\eta G^{\frac{2}{p-1}}}{2}$$

where n_t is the batch size in iteration t and L, $\vec{\sigma}$, and G are constants from Assumption 1, 3, 4. Further letting the batch size $n_t = T$, the number of gradient call is $N = T^2$ for T iterations. With $\eta = \frac{1}{L^{\frac{1}{2}}G^{\frac{1}{p-1}}T^{\frac{1}{2}}}$ we have

$$\mathbb{E}\left[\frac{1}{T}\sum_{t=0}^{T-1}\|\nabla f(\theta_t)\|_{p^*}^{p^*}\right] \leq \frac{1}{N^{\frac{1}{4}}}\left[L^{\frac{1}{2}}G^{\frac{1}{p-1}}\left(f(\theta_0)-f(\theta^*)+\frac{1}{2}\right)+\frac{2p-1}{p-1}G^{\frac{1}{p-1}}\|\vec{\sigma}\|_1\right],$$

i.e., Algorithm 1 takes $N \in \mathcal{O}\left(\epsilon^{-4}\right)$ gradient queries to reach an ϵ-approximate stationary point.

Proof. Starting with Assumption 1 and the descent step in Algorithm 1,

$$\begin{aligned}
f(\theta_{t+1}) &\leq f(\theta_t) + \langle \nabla f(\theta_t),\, \theta_{t+1}-\theta_t\rangle + \frac{L}{2}\|\theta_{t+1}-\theta_t\|_p^2 \\
&= f(\theta_t) + \eta\,\langle \nabla f(\theta_t),\, -s(g(\theta_t))\rangle + \frac{L}{2}\|s(g(\theta_t))\|_p^2 \\
&= f(\theta_t) - \underbrace{\eta\,\langle \nabla f(\theta_t),\, s(\nabla f(\theta_t))\rangle}_{A} \\
&\quad + \underbrace{\eta\,\langle \nabla f(\theta_t),\, s(\nabla f(\theta_t)) - s(g(\theta_t))\rangle}_{B} + \underbrace{\frac{L\eta^2}{2}\|s(g(\theta_t))\|_p^2}_{C}
\end{aligned}$$

Now we analyze these terms one by one.

$$\begin{aligned}
A &= \sum_{i=1}^{d}\nabla f(\theta_t)^{(i)}\cdot\frac{\nabla f(\theta_t)^{(i)}}{|\nabla f(\theta_t)^{(i)}|^{\frac{p-2}{p-1}}} \\
&= \sum_{i=1}^{d}|\nabla f(\theta_t)^{(i)}|^{\frac{p}{p-1}} \\
&= \|\nabla f(\theta_t)\|_{p^*}^{p^*}
\end{aligned}$$

For term B,

$$\begin{aligned}
B &= \eta\sum_{i=1}^{d}\nabla f(\theta_t)^{(i)}\left(\frac{\nabla f(\theta_t)^{(i)}}{|\nabla f(\theta_t)^{(i)}|^{\frac{p-2}{p-1}}} - \frac{g(\theta_t)^{(i)}}{|g(\theta_t)^{(i)}|^{\frac{p-2}{p-1}}}\right) \\
&= \eta\sum_{i=1}^{d}\nabla f(\theta_t)^{(i)}\left(\text{sign}\left(\nabla f(\theta_t)^{(i)}\right)|\nabla f(\theta_t)^{(i)}|^{\frac{1}{p-1}} - \text{sign}\left(g(\theta_t)^{(i)}\right)|g(\theta_t)^{(i)}|^{\frac{1}{p-1}}\right) \\
&\leq \eta\sum_{i=1}^{d}\left|\nabla f(\theta_t)^{(i)}\right|\left|\text{sign}\left(\nabla f(\theta_t)^{(i)}\right)|\nabla f(\theta_t)^{(i)}|^{\frac{1}{p-1}} - \text{sign}\left(g(\theta_t)^{(i)}\right)|g(\theta_t)^{(i)}|^{\frac{1}{p-1}}\right| \\
&= \underbrace{\eta\sum_{i=1}^{d}\left|\nabla f(\theta_t)^{(i)}\right|\left(|\nabla f(\theta_t)^{(i)}|^{\frac{1}{p-1}} + |g(\theta_t)^{(i)}|^{\frac{1}{p-1}}\right)\mathbb{I}\left[\text{sign}\left(\nabla f(\theta_t)^{(i)}\right)\neq\text{sign}\left(g(\theta_t)^{(i)}\right)\right]}_{B_1} \\
&\quad + \underbrace{\eta\sum_{i=1}^{d}\left|\nabla f(\theta_t)^{(i)}\right|\left||\nabla f(\theta_t)^{(i)}|^{\frac{1}{p-1}} - |g(\theta_t)^{(i)}|^{\frac{1}{p-1}}\right|\mathbb{I}\left[\text{sign}\left(\nabla f(\theta_t)^{(i)}\right)=\text{sign}\left(g(\theta_t)^{(i)}\right)\right]}_{B_2}
\end{aligned}$$

B_1 is bounded in expectation by $\frac{2\eta G^{\frac{1}{p-1}}\|\vec{\sigma}\|_1}{\sqrt{n_t}}$ in Lemma 2 and B_2 is bounded in expectation by $\frac{\eta G^{\frac{1}{p-1}}\|\vec{\sigma}\|_1}{(p-1)\sqrt{n_t}}$ in Lemma 3.

$$\begin{aligned}
C &= \frac{L\eta^2}{2}\left(\sum_{i=1}^{d}\left|\frac{\nabla f(\theta_t)^{(i)}}{|\nabla f(\theta_t)^{(i)}|^{\frac{p-2}{p-1}}}\right|^p\right)^{\frac{2}{p}} \\
&= \frac{L\eta^2}{2}\left(\sum_{i=1}^{d}\left|\nabla f(\theta_t)^{(i)}\right|^{\frac{p}{p-1}}\right)^{\frac{2}{p}} \\
&= \frac{L\eta^2}{2}\|\nabla f(\theta_t)\|_{p^*}^{\frac{2}{p-1}} \\
&\leq \frac{L\eta^2 G^{\frac{2}{p-1}}}{2}
\end{aligned}$$

Therefore,

$$\eta\mathbb{E}\left[\|\nabla f(\theta_t)\|_{p^*}^{p^*}\right] \leq f(\theta_t) - f(\theta_{t+1}) + \frac{\eta(2p-1)G^{\frac{1}{p-1}}\|\vec{\sigma}\|_1}{(p-1)\sqrt{n_t}} + \frac{L\eta^2 G^{\frac{2}{p-1}}}{2}$$

By telescoping through $t = 0, \cdots, T-1$, we get

$$\mathbb{E}\left[\frac{1}{T}\sum_{t=0}^{T-1}\|\nabla f(\theta_t)\|_{p^*}^{p^*}\right] \leq \frac{f(\theta_0) - f(\theta_T)}{\eta T} + \frac{1}{T}\sum_{t=0}^{T-1}\frac{(2p-1)G^{\frac{1}{p-1}}\|\vec{\sigma}\|_1}{(p-1)\sqrt{n_t}} + \frac{L\eta G^{\frac{2}{p-1}}}{2}$$

□

Lemma 2.

$$\mathbb{E}\left[\eta\sum_{i=1}^{d}\left|\nabla f(\theta_t)^{(i)}\right|\left(|\nabla f(\theta_t)^{(i)}|^{\frac{1}{p-1}} + |g(\theta_t)^{(i)}|^{\frac{1}{p-1}}\right)\mathbb{I}\left[\operatorname{sign}\left(\nabla f(\theta_t)^{(i)}\right) \neq \operatorname{sign}\left(g(\theta_t)^{(i)}\right)\right]\right] \leq \frac{2\eta G^{\frac{1}{p-1}}\|\vec{\sigma}\|_1}{\sqrt{n_t}}$$

Proof. By Corollary 3 (b),

$$\begin{aligned}
&\mathbb{E}\left[\eta\sum_{i=1}^{d}\left|\nabla f(\theta_t)^{(i)}\right|\left(|\nabla f(\theta_t)^{(i)}|^{\frac{1}{p-1}} + |g(\theta_t)^{(i)}|^{\frac{1}{p-1}}\right)\mathbb{I}\left[\operatorname{sign}\left(\nabla f(\theta_t)^{(i)}\right) \neq \operatorname{sign}\left(g(\theta_t)^{(i)}\right)\right]\right] \\
&\leq 2\eta G^{\frac{1}{p-1}}\,\mathbb{E}\left[\sum_{i=1}^{d}\left|\nabla f(\theta_t)^{(i)}\right|\mathbb{I}\left[\operatorname{sign}\left(\nabla f(\theta_t)^{(i)}\right) \neq \operatorname{sign}\left(g(\theta_t)^{(i)}\right)\right]\right] \\
&= 2\eta G^{\frac{1}{p-1}}\sum_{i=1}^{d}\left|\nabla f(\theta_t)^{(i)}\right|\mathbb{P}\left[\operatorname{sign}\left(\nabla f(\theta_t)^{(i)}\right) \neq \operatorname{sign}\left(g(\theta_t)^{(i)}\right)\right] \\
&\leq 2\eta G^{\frac{1}{p-1}}\sum_{i=1}^{d}\left|\nabla f(\theta_t)^{(i)}\right|\mathbb{P}\left[\left|g(\theta_t)^{(i)} - \nabla f(\theta_t)^{(i)}\right| \geq \left|\nabla f(\theta_t)^{(i)}\right|\right] \\
&\leq 2\eta G^{\frac{1}{p-1}}\sum_{i=1}^{d}\left|\nabla f(\theta_t)^{(i)}\right|\frac{\mathbb{E}\left[\left|g(\theta_t)^{(i)} - \nabla f(\theta_t)^{(i)}\right|\right]}{|\nabla f(\theta_t)^{(i)}|} \\
&\leq 2\eta G^{\frac{1}{p-1}}\sum_{i=1}^{d}\sqrt{\mathbb{E}\left[|g(\theta_t)^{(i)} - \nabla f(\theta_t)^{(i)}|^2\right]} \\
&\leq \frac{2\eta G^{\frac{1}{p-1}}\sum_{i=1}^{d}\sigma_i}{\sqrt{n_t}} \\
&= \frac{2\eta G^{\frac{1}{p-1}}\|\vec{\sigma}\|_1}{\sqrt{n_t}}
\end{aligned}$$

where for the last three inequalities we used Markov's inequality, Jensen's inequality, and Assumption 3. □

Lemma 3.

$$\mathbb{E}\left[\eta\sum_{i=1}^{d}\left|\nabla f(\theta_t)^{(i)}\right|\left||\nabla f(\theta_t)^{(i)}|^{\frac{1}{p-1}} - |g(\theta_t)^{(i)}|^{\frac{1}{p-1}}\right|\mathbb{I}\left[\operatorname{sign}\left(\nabla f(\theta_t)^{(i)}\right) = \operatorname{sign}\left(g(\theta_t)^{(i)}\right)\right]\right] \leq \frac{\eta G^{\frac{1}{p-1}}\|\vec{\sigma}\|_1}{(p-1)\sqrt{n_t}}$$

Proof. Denoting $\mathbb{E}\left[\cdot \mid \operatorname{sign}\left(\nabla f(\theta_t)^{(i)}\right) = \operatorname{sign}\left(g(\theta_t)^{(i)}\right)\right]$ as $\mathbb{E}_{|=}[\cdot]$, and $\mathbb{P}\left[\operatorname{sign}\left(\nabla f(\theta_t)^{(i)}\right) = \operatorname{sign}\left(g(\theta_t)^{(i)}\right)\right]$ as $\mathbb{P}\left[=\right]$,

$$
\begin{aligned}
&\mathbb{E}\left[\eta \sum_{i=1}^{d} \left|\nabla f(\theta_t)^{(i)}\right| \left||\nabla f(\theta_t)^{(i)}|^{\frac{1}{p-1}} - |g(\theta_t)^{(i)}|^{\frac{1}{p-1}}\right| \mathbb{I}\left[\operatorname{sign}\left(\nabla f(\theta_t)^{(i)}\right) = \operatorname{sign}\left(g(\theta_t)^{(i)}\right)\right]\right] \\
&= \eta \mathbb{E}_{|=}\left[\sum_{i=1}^{d} \left|\nabla f(\theta_t)^{(i)}\right| \left||\nabla f(\theta_t)^{(i)}|^{\frac{1}{p-1}} - |g(\theta_t)^{(i)}|^{\frac{1}{p-1}}\right|\right] \mathbb{P}\left[=\right] \\
&= \eta \mathbb{E}_{|=}\left[\sum_{i=1}^{d} \left|\nabla f(\theta_t)^{(i)}\right| \left||\nabla f(\theta_t)^{(i)}|^{\frac{1}{p-1}} - |g(\theta_t)^{(i)}|^{\frac{1}{p-1}}\right|\right] \mathbb{P}\left[=\right] \\
&= \eta \mathbb{E}_{|=}\left[\sum_{i=1}^{d} \left|\nabla f(\theta_t)^{(i)}\right| \left|\left(|g(\theta_t)^{(i)}|^{\frac{1}{p-1}} + \frac{1}{p-1} \operatorname{sign}(\zeta^{(i)}) \left|\zeta^{(i)}\right|^{\frac{2-p}{p-1}} \left(\nabla f(\theta_t)^{(i)} - g(\theta_t)^{(i)}\right)\right) - |g(\theta_t)^{(i)}|^{\frac{1}{p-1}}\right|\right] \mathbb{P}\left[=\right] \\
&= \eta \mathbb{E}_{|=}\left[\sum_{i=1}^{d} \left|\nabla f(\theta_t)^{(i)}\right| \left|\frac{1}{p-1} \operatorname{sign}(\zeta^{(i)}) \left|\zeta^{(i)}\right|^{\frac{2-p}{p-1}} \left(\nabla f(\theta_t)^{(i)} - g(\theta_t)^{(i)}\right)\right|\right] \mathbb{P}\left[=\right] \\
&= \frac{\eta}{p-1} \mathbb{E}_{|=}\left[\sum_{i=1}^{d} \left|\nabla f(\theta_t)^{(i)}\right| \left|\zeta^{(i)}\right|^{\frac{2-p}{p-1}} \left|\nabla f(\theta_t)^{(i)} - g(\theta_t)^{(i)}\right|\right] \mathbb{P}\left[=\right],
\end{aligned}
$$

in which the second equality holds by taking the zeroth order Taylor expansion of $\left|\nabla f(\theta_t)^{(i)}\right|^{\frac{1}{p-1}}$ at $g(\theta_t)^{(i)}$ with Lagrange remainder, and $\zeta^{(i)}$ is in the range from $\nabla f(\theta_t)^{(i)}$ to $g(\theta_t)^{(i)}$.

Given $\operatorname{sign}\left(\nabla f(\theta_t)^{(i)}\right) = \operatorname{sign}\left(g(\theta_t)^{(i)}\right)$, by the definition of $\zeta^{(i)}$ in the Lagrange remainder, we must have either $\left|\nabla f(\theta_t)^{(i)}\right| \le \left|\zeta^{(i)}\right| \le \left|g(\theta_t)^{(i)}\right|$ or $\left|\nabla f(\theta_t)^{(i)}\right| \ge \left|\zeta^{(i)}\right| \ge \left|g(\theta_t)^{(i)}\right|$. Now we analyze these two cases respectively. We write out the derivations separately for clarity and simplicity, alternatively one can merge these two cases with the law of total expectation.

(1) If $\left|\nabla f(\theta_t)^{(i)}\right| \le \left|\zeta^{(i)}\right| \le \left|g(\theta_t)^{(i)}\right|$, then

$$
\begin{aligned}
\frac{\eta}{p-1} \mathbb{E}_{|=}&\left[\sum_{i=1}^{d} \left|\nabla f(\theta_t)^{(i)}\right| \left|\zeta^{(i)}\right|^{\frac{2-p}{p-1}} \left|\nabla f(\theta_t)^{(i)} - g(\theta_t)^{(i)}\right|\right] \mathbb{P}\left[=\right] \\
&\le \frac{\eta}{p-1} \mathbb{E}_{|=}\left[\sum_{i=1}^{d} \left|\zeta^{(i)}\right| \left|\zeta^{(i)}\right|^{\frac{2-p}{p-1}} \left|\nabla f(\theta_t)^{(i)} - g(\theta_t)^{(i)}\right|\right] \mathbb{P}\left[=\right] \\
&= \frac{\eta}{p-1} \mathbb{E}_{|=}\left[\sum_{i=1}^{d} \left|\zeta^{(i)}\right|^{\frac{1}{p-1}} \left|\nabla f(\theta_t)^{(i)} - g(\theta_t)^{(i)}\right|\right] \mathbb{P}\left[=\right] \\
&\le \frac{\eta}{p-1} \mathbb{E}_{|=}\left[\sum_{i=1}^{d} \left|g(\theta_t)^{(i)}\right|^{\frac{1}{p-1}} \left|\nabla f(\theta_t)^{(i)} - g(\theta_t)^{(i)}\right|\right] \mathbb{P}\left[=\right] \\
&\le \frac{\eta G^{\frac{1}{p-1}}}{p-1} \sum_{i=1}^{d} \mathbb{E}_{|=}\left[\left|\nabla f(\theta_t)^{(i)} - g(\theta_t)^{(i)}\right|\right] \mathbb{P}\left[=\right] \\
&= \frac{\eta G^{\frac{1}{p-1}}}{p-1} \sum_{i=1}^{d} \frac{\mathbb{E}\left[\left|\nabla f(\theta_t)^{(i)} - g(\theta_t)^{(i)}\right|\right]}{\mathbb{P}[=]} \mathbb{P}\left[=\right] \\
&\le \frac{\eta G^{\frac{1}{p-1}}}{p-1} \sum_{i=1}^{d} \sqrt{\mathbb{E}\left[|\nabla f(\theta_t)^{(i)} - g(\theta_t)^{(i)}|^2\right]} && \text{(Jensen's)} \\
&\le \frac{\eta G^{\frac{1}{p-1}}}{p-1} \sum_{i=1}^{d} \frac{\sigma_i}{\sqrt{n_t}} && \text{(Assumption 3)} \\
&= \frac{\eta G^{\frac{1}{p-1}} \|\vec{\sigma}\|_1}{(p-1)\sqrt{n_t}}
\end{aligned}
$$

(2) If $\left|\nabla f(\theta_t)^{(i)}\right| \geq \left|\zeta^{(i)}\right| \geq \left|g(\theta_t)^{(i)}\right|$, then

$$
\begin{aligned}
&\frac{\eta}{p-1}\mathbb{E}_{|=}\left[\sum_{i=1}^{d}\left|\nabla f(\theta_t)^{(i)}\right|\left|\zeta^{(i)}\right|^{\frac{2-p}{p-1}}\left|\nabla f(\theta_t)^{(i)} - g(\theta_t)^{(i)}\right|\right]\mathbb{P}\left[=\right] \\
&\leq \frac{\eta}{p-1}\mathbb{E}_{|=}\left[\sum_{i=1}^{d}\left|\nabla f(\theta_t)^{(i)}\right|\left|g(\theta_t)^{(i)}\right|^{\frac{2-p}{p-1}}\left|\nabla f(\theta_t)^{(i)} - g(\theta_t)^{(i)}\right|\right]\mathbb{P}\left[=\right] \\
&\leq \frac{\eta}{(p-1)\mathbb{P}[=]}\mathbb{E}\left[\sum_{i=1}^{d}\left|\nabla f(\theta_t)^{(i)}\right|\left|g(\theta_t)^{(i)}\right|^{\frac{2-p}{p-1}}\left|\nabla f(\theta_t)^{(i)} - g(\theta_t)^{(i)}\right|\right]\mathbb{P}\left[=\right] \\
&\leq \frac{\eta}{p-1}\sum_{i=1}^{d}\sqrt{\mathbb{E}\left[|\nabla f(\theta_t)^{(i)}|^2\,|g(\theta_t)^{(i)}|^{\frac{2(2-p)}{p-1}}\right]\mathbb{E}\left[|\nabla f(\theta_t)^{(i)} - g(\theta_t)^{(i)}|^2\right]} && \text{(Cauchy-Schwarz)} \\
&\leq \frac{\eta}{p-1}\sum_{i=1}^{d}\sqrt{|\nabla f(\theta_t)^{(i)}|^2\,\mathbb{E}\left[|g(\theta_t)^{(i)}|^{\frac{2(2-p)}{p-1}}\right]\frac{\sigma_i^2}{n_t}} && \text{(Assumption 3)} \\
&\leq \frac{\eta}{p-1}\sum_{i=1}^{d}\sqrt{|\nabla f(\theta_t)^{(i)}|^2\left(\mathbb{E}\left[|g(\theta_t)^{(i)}|^2\right]\right)^{\frac{2-p}{p-1}}\frac{\sigma_i^2}{n_t}} && \text{(Jensen's)} \\
&\leq \frac{\eta}{p-1}\sum_{i=1}^{d}\sqrt{|\nabla f(\theta_t)^{(i)}|^2\left(\mathrm{Var}\left[g(\theta_t)^{(i)}\right] + \left(\mathbb{E}\left[g(\theta_t)^{(i)}\right]\right)^2\right)^{\frac{2-p}{p-1}}\frac{\sigma_i^2}{n_t}} && \text{(Variance Definition)} \\
&\leq \frac{\eta}{p-1}\sum_{i=1}^{d}\sqrt{|\nabla f(\theta_t)^{(i)}|^2\left(\mathbb{E}\left[g(\theta_t)^{(i)}\right]\right)^{\frac{2(2-p)}{p-1}}\frac{\sigma_i^2}{n_t}} \\
&= \frac{\eta}{p-1}\sum_{i=1}^{d}\left|\nabla f(\theta_t)^{(i)}\right|^{\frac{1}{p-1}}\frac{\sigma_i}{\sqrt{n_t}} && \text{(Assumption 2)} \\
&\leq \frac{\eta G^{\frac{1}{p-1}}\|\vec{\sigma}\|_1}{(p-1)\sqrt{n_t}}.
\end{aligned}
$$

Combining these two cases together (e.g. by the law of total expectation) completes the proof.

□

B ℓ_2 Majorization and ℓ_p Smoothness

Another assumption of interest, as studied by Bernstein et al. (2018) (as well as Karimi et al. (2016)), is that of ℓ_2 *majorization* (with respect to $\vec{L} = [L_1, \ldots, L_d]$), meaning that for all $x, y \in \mathbb{R}^d$,

$$\left|f(y) - f(x) - \nabla f(x)^\top (y-x)\right| \leq \frac{1}{2}\sum_{i=1}^{d} L_i (y^{(i)} - x^{(i)})^2.$$

We may equivalently express this condition as 1-smoothness w.r.t. $\|\cdot\|_{\mathbf{L}}$, where $\mathbf{L} := \mathrm{diag}(\vec{L})$, i.e., for all $x, y \in \mathbb{R}^d$, $\|\nabla f(y) - \nabla f(x)\|_{\mathbf{L}^{-1}} \leq \|y - x\|_{\mathbf{L}}$.

Interestingly, we may observe that, for any $1 \leq p \leq \infty$,

$$\frac{1}{\|\vec{L}\|_{p^*}^{1/2}}\|\nabla f(y) - \nabla f(x)\|_{2p/(2p-1)} \leq \|\nabla f(y) - \nabla f(x)\|_{\mathbf{L}^{-1}} \leq \|y - x\|_{\mathbf{L}} \leq \|\vec{L}\|_{p^*}^{1/2}\|y - x\|_{2p},$$

where the first inequality holds by reverse Hölder's inequality, i.e., for $u, v \in \mathbb{R}^d$, $\sum_{i=1}^{d}|u^{(i)}v^{(i)}| \geq \|u\|_{1/q}\|v\|_{\frac{-1}{q-1}}$ (where we choose $q = \frac{2p-1}{p}$), and the last inequality holds by Hölder's inequality.

Rearranging, we have $\|\nabla f(y) - \nabla f(x)\|_{2p/(2p-1)} \leq \|\vec{L}\|_{p^*}\|y - x\|_{2p}$, and so it follows that ℓ_2 majorization implies $\|\vec{L}\|_{\frac{p}{p-2}}$-smoothness w.r.t. $\|\cdot\|_p$. Thus, while this condition is sufficient to entail ℓ_p smoothness (as previously noted by Balles et al. (2020) in the case of $p = \infty$), we nevertheless prefer to work directly with ℓ_p smoothness assumptions, as we believe they provide a more natural pairing for the methods we consider.

Table 3: Image classification on CIFAR at the 50th, 100th, and 200th epochs. STACEY$_{(2,p)}$ consistently lower performance than STACEY$_{(p,p)}$ at all epochs.

Optimizer	Training NLL ↓			Testing ACC (%) ↑		
	@50 epoch	@100 epoch	@200 epoch	@50 epoch	@100 epoch	@200 epoch
STACEY$_{(2,p)}$	0.1017	0.0365	0.0083	90.78	91.88	93.55
STACEY$_{(p,p)}$	0.1438	0.0405	0.0006	88.95	91.50	**94.05**
STACEY$_{(p,2)}$	**0.0375**	**0.0104**	**0.0005**	**91.87**	**92.92**	93.99

Table 4: Image classification on ImageNet at the 20th, 50th, and 90th epochs. STACEY$_{(2,p)}$ consistently lower performance than STACEY$_{(p,p)}$ at all epochs.

Optimizer	Training NLL ↓			Testing Top-1 ACC (%) ↑		
	@20 epoch	@50 epoch	@90 epoch	@20 epoch	@50 epoch	@90 epoch
STACEY$_{(2,p)}$	2.5178	1.8038	1.4274	50.59	61.72	65.11
STACEY$_{(p,p)}$	**1.9371**	**1.2064**	**0.9902**	**60.84**	**68.23**	**69.88**
STACEY$_{(p,2)}$	3.3706	2.5149	2.1975	32.16	49.39	57.33

C THE VARIATION STACEY$_{(2,p)}$

For the sake of completion, we also considered the (natural) variant STACEY$_{(2,p)}$, which couples ℓ_2 steepest descent with mirror descent (for dgf $\frac{1}{p}\|\cdot\|_p^p$).

Algorithm 4 STACEY$_{(2,p)}$ Optimizer

```
input $p, \beta_1, \beta_2, \alpha, \tau, \eta, \epsilon, \lambda, f$
initialize $\theta_0, z_0, m_0 \leftarrow 0$
while $\theta_{t+1}$ not converged do
    $g_t \leftarrow g(\theta_t)$
    $c_{t+1} \leftarrow \beta_1 m_t + (1-\beta_1) g_t$
    $y_{t+1} \leftarrow \theta_t - \eta_t c_{t+1}$
    $z_{t+1}^{(i)} = \frac{\left|z_t^{(i)}\right|^{p-2} z_t^{(i)} - \alpha c_{t+1}^{(i)}}{\left|\left|z_t^{(i)}\right|^{p-2} z_t^{(i)} - \alpha c_{t+1}^{(i)}\right|^{\frac{p-2}{p-1}}}, \forall\, i \in [d]$
    $\theta_{t+1} = \tau z_{t+1} + (1-\tau) y_{t+1} - \eta_t \lambda \theta_t$
    $m_{t+1} = \beta_2 m_t + (1-\beta_2) g_t$
return $\theta_{t+1}$
```

Table 3&4 show the classification results of STACEY$_{(2,p)}$ optimizer. The experimental results of STACEY$_{(2,p)}$ optimizer with varying p-norm are shown in Appendix E. Specifically, the results on CIFAR (Krizhevsky, 2009) are shown in Fig. 6a&7a, the results on ImageNet (Deng et al., 2009) are shown in Fig. 8a&9a&10a, and the results on LLM pertaining are shown in Fig. 11a&12a&13a.

D HYPER-PARAMETER CHOICES

We list the hyper-parameters used in the experiments in Table 5&6&7, which are determined by grid search. We employ Weight & Bias platform[10] to tune the hyper-parameters. To ensure a fair comparison, the experimental settings beyond the listed hyper-parameters remain the same for all optimizers. For example, the data augmentation for ImageNet (Deng et al., 2009) and CIFAR (Krizhevsky, 2009) is random cropping plus random horizontal flipping.

[10] https://github.com/wandb/wandb.

Table 5: CIFAR hyper-parameters.

Model	**Optimizer**	**Batch Size**	p	lr (η)	α	β_1	β_2	λ	τ	ϵ
ResNet-18	SGD w/ Nesterov	128	-	0.02	-	0.9	-	0.0002	-	-
ResNet-18	Adam	128	-	0.001	-	0.9	0.999	0.0005	-	1e-8
ResNet-18	AdamW	128	-	0.01	-	0.9	0.999	0.0005	-	1e-8
ResNet-18	Lion	128	-	0.001	-	0.9	0.99	0.01	-	-
ResNet-18	STACEY$_{(2,p)}$	128	3.5	0.02	0.01	0.9	0.99	0.4	0.001	-
ResNet-18	STACEY$_{(p,p)}$	128	2	0.1	0.1	0.9	0.99	0.01	0.001	1e-12
ResNet-18	STACEY$_{(p,2)}$	128	2	0.1	0.1	0.9	0.99	0.01	0.001	1e-12

Table 6: ImageNet hyper-parameters.

Model	**Optimizer**	**Batch Size**	p	lr (η)	α	β_1	β_2	λ	τ	ϵ
ResNet-50	SGD w/ Nesterov	256	-	0.01	-	-	-	0.0005	-	-
ResNet-50	STACEY$_{(2,p)}$	256	2.2	0.01	0.01	0.9	0.99	0.0005	0.001	-
ResNet-50	STACEY$_{(p,p)}$	256	3	0.01	0.1	0.9	0.99	0.0005	0.001	1e-8
ResNet-50	STACEY$_{(p,2)}$	256	2.8	0.01	0.01	0.9	0.99	0.0005	0.001	1e-8

E ADDITIONAL EXPERIMENTAL RESULTS

E.1 LEARNING CURVES OF VARYING ℓ_p-NORM ON CIFAR CLASSIFICATION

The results are shown in Fig. 6&7.

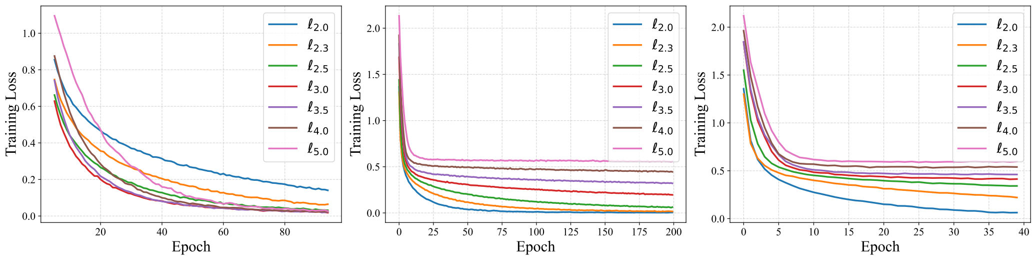

(a) STACEY$_{(2,p)}$ (b) STACEY$_{(p,p)}$ (c) STACEY$_{(p,2)}$

Figure 6: Training loss of CIFAR classification with varying ℓ_p-norm.

E.2 LEARNING CURVES OF VARYING ℓ_p-NORM ON IMAGENET CLASSIFICATION

The results are shown in Fig. 8&9&10.

E.3 LEARNING CURVES OF VARYING ℓ_p-NORM ON LLM PRETRAINING

The results are shown in Fig. 11&12&13.

Table 7: Hyper-parameters for LLM pretraining.

Model	**Optimizer**	**Batch Size**	p	lr (η)	α	β_1	β_2	λ	τ	ϵ
Llama 100M	SGD	16	-	0.01	-	-	-	0.0005	-	-
Llama 100M	Adam	16	-	0.0001	-	0.9	0.999	0.01	-	1e-8
Llama 100M	AdamW	16	-	0.0001	-	0.9	0.999	0.05	-	1e-8
Llama 100M	Lion	16	-	0.05	-	0.9	0.999	0.01	-	-
Llama 100M	STACEY$_{(2,p)}$	16	2.8	0.05	0.01	0.9	0.99	0.01	0.001	-
Llama 100M	STACEY$_{(p,p)}$	16	3	0.01	0.01	0.9	0.99	0.01	0.001	1e-8
Llama 100M	STACEY$_{(p,2)}$	16	2.8	0.01	0.01	0.9	0.99	0.0005	0.001	1e-8

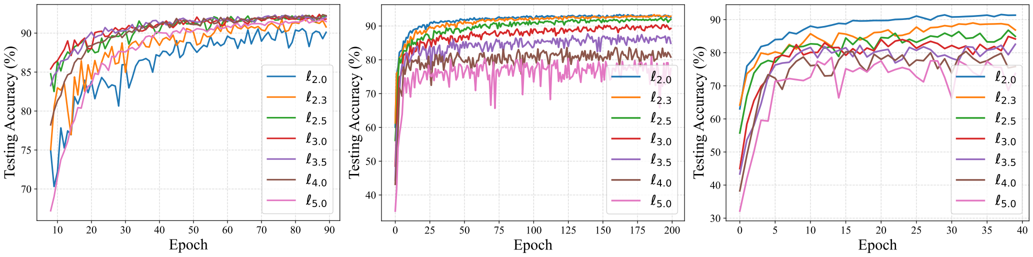

(a) STACEY$_{(2,p)}$ (b) STACEY$_{(p,p)}$ (c) STACEY$_{(p,2)}$

Figure 7: Testing accuracy of CIFAR classification with varying ℓ_p-norm.

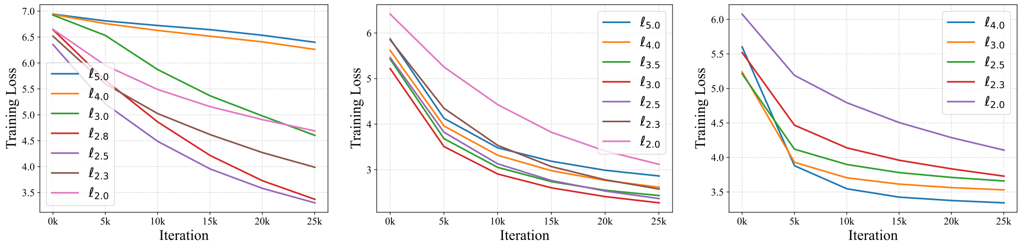

(a) STACEY$_{(2,p)}$ (b) STACEY$_{(p,p)}$ (c) STACEY$_{(p,2)}$

Figure 8: Training loss of ImageNet classification with varying ℓ_p-norm.

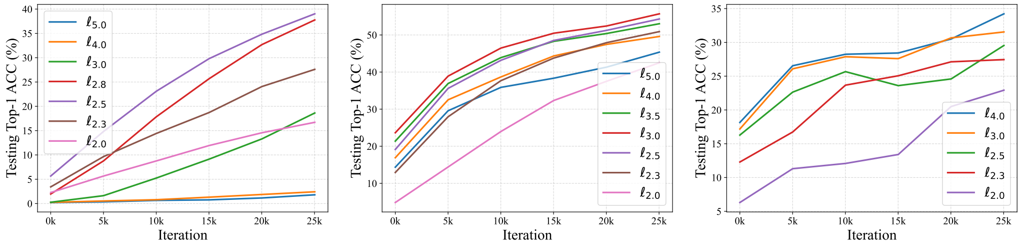

(a) STACEY$_{(2,p)}$ (b) STACEY$_{(p,p)}$ (c) STACEY$_{(p,2)}$

Figure 9: Testing Top-1 accuracy of ImageNet classification with varying ℓ_p-norm.

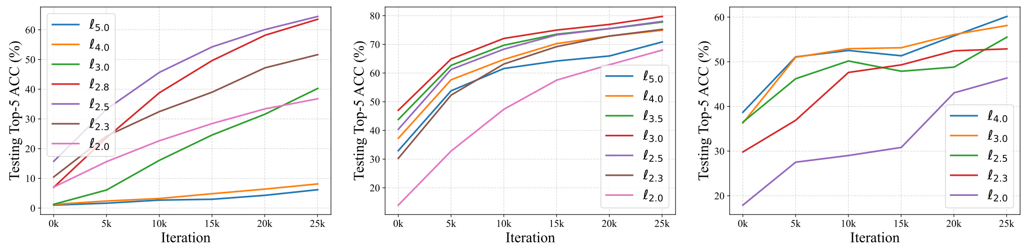

(a) STACEY$_{(2,p)}$ (b) STACEY$_{(p,p)}$ (c) STACEY$_{(p,2)}$

Figure 10: Testing Top-5 accuracy of ImageNet classification with varying ℓ_p-norm.

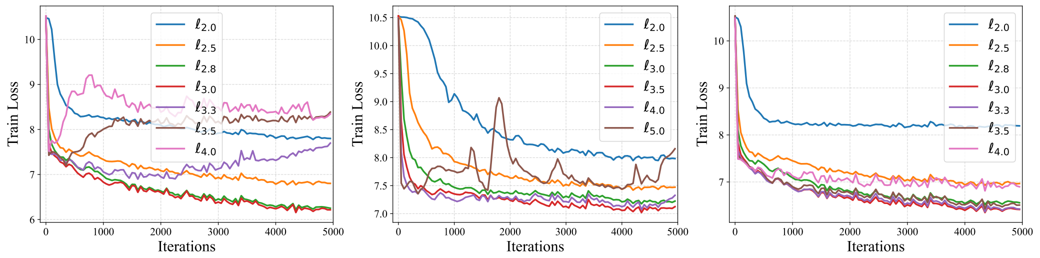

(a) STACEY$_{(2,p)}$ (b) STACEY$_{(p,p)}$ (c) STACEY$_{(p,2)}$

Figure 11: Training loss of pretraining Llama on C4 dataset with varying ℓ_p-norm.

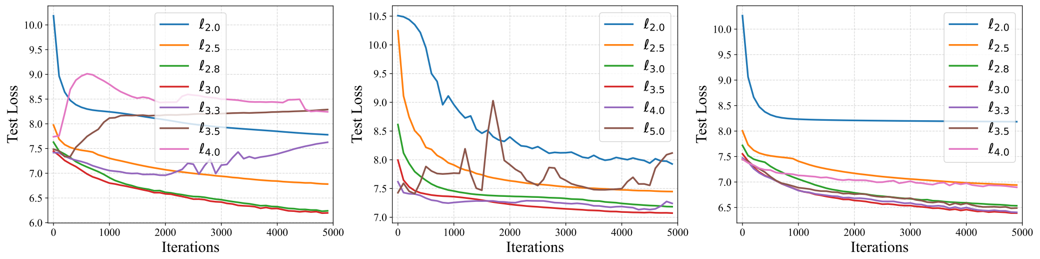

(a) STACEY$_{(2,p)}$ (b) STACEY$_{(p,p)}$ (c) STACEY$_{(p,2)}$

Figure 12: Testing loss of pretraining Llama on C4 dataset with varying ℓ_p-norm.

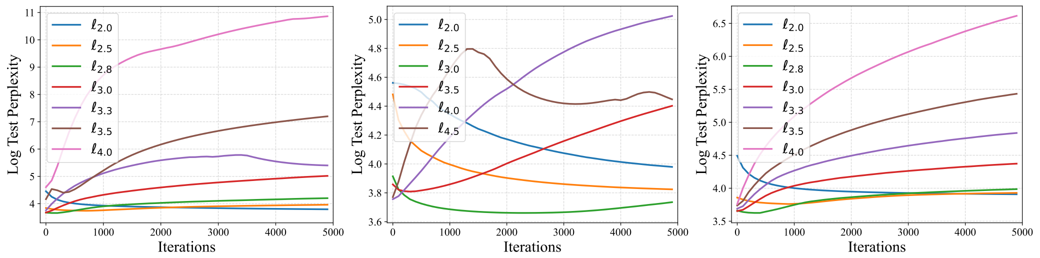

(a) STACEY$_{(2,p)}$ (b) STACEY$_{(p,p)}$ (c) STACEY$_{(p,2)}$

Figure 13: Log testing perplexity of pretraining Llama on C4 dataset with varying ℓ_p-norm.